Title: Carbon cycling in mature and regrowth forests globally

Summary

Background. Forests are major components of the global carbon (C) cycle and thereby strongly influence atmospheric carbon dioxide (CO_2) and climate. However, efforts to incorporate forests into climate models and CO_2 accounting frameworks have been constrained by a lack of accessible, global-scale synthesis on how C cycling varies across forest types and stand ages.

Methods/Design. Here, we draw from the Global Forest Carbon Database, ForC, to provide a macroscopic overview of C cycling in the world's forests, giving special attention to stand age-related variation. Specifically, we use 11923 *ForC* records for 34 C cycle variables from 865 geographic locations to characterize ensemble C budgets for four broad forest types – tropical broadleaf evergreen, temperate broadleaf, temperate conifer, and boreal. We calculate means and standard deviations for both mature and regrowth (age <100 years) forests and quantify trends with stand age in regrowth forests for all variables with sufficient data.

Review Results/ Synthesis. C cycling rates generally decreased from tropical to temperate to boreal in both mature and regrowth forests, whereas C stocks showed less directional variation. Mature forest net ecosystem production did not differ significantly among biomes. The majority of flux variables, together with most live biomass pools, increased significantly with the logarithm of stand age.

Discussion. As climate change accelerates, understanding and managing the carbon dynamics of forests is critical to forecasting, mitigation, and adaptation. This comprehensive and synthetic global overview of C stocks and fluxes across biomes and stand ages contributes to these efforts.

Key words: forest ecosystems; carbon cycle; stand age; productivity; respiration; biomass; global

Background

Forest ecosystems are shaping the course of climate change through their influence on atmospheric carbon dioxide, CO_2 (Bonan 2008, IPCC 2018, Friedlingstein *et al* 2019). Despite the centrality of forest C cycling in regulating atmospheric CO_2, gaps in our understanding of how C cycling varies across forest types and in relation to stand history underly important uncertainties in climate models (Friedlingstein *et al* 2006, Krause *et al* 2018, Bonan *et al* 2019, Di Vittorio *et al* 2020) and CO_2 accounting frameworks (Pan *et al* 2011, IPCC 2019). Improved understanding of forest C cycling globally require accessible, comprehensive, and large-scale databases with worldwide coverage, which runs contrary to the traditional way forest C stocks and fluxes have been measured and published. Large-scale synthesis is critical to benchmarking model performance with global data (Luo *et al* 2012, Clark *et al* 2017, Fer *et al* 2021), quantifying the role of forests in the global C cycle (e.g., Pan *et al* 2011, Harris *et al* 2021), and using book-keeping methods to quantify actual or potential exchanges of CO_2 between forests and the atmosphere (Griscom *et al* 2017, Houghton 2020).

Forests in the global C cycle: current and future

A robust understanding of forest impacts on global C cycling is essential. Total annual photosynthesis in forests (gross primary productivity, GPP) is estimated at approximately 69 Gt C yr^{-1} (Badgley *et al* 2019). Most of this enormous C uptake is counterbalanced by releases to the atmosphere through ecosystem respiration (R_{eco}) and fire. In recent years, total forest C uptake has exceeded releases, such that forests globally have been a C sink (Harris *et al* 2021). This C sink has averaged 3.2 ± 0.6 Gt C yr^{-1} for 2009-2018, offsetting 29% of anthropogenic fossil fuel emissions, when considering only areas remaining forested (Friedlingstein *et al* 2019). However, deforestation, estimated at ~1 Gt C yr^{-1} in recent decades (Pan *et al* 2011, Tubiello *et al* 2020), reduces the net forest sink to ~1.1-2.2 Gt C yr^{-1} (Friedlingstein *et al* 2019, Harris *et al* 2021). Understanding, modeling, and managing forest-atmosphere CO2 exchange is central to mitigating climate change (Cavaleri *et al* 2015, Grassi *et al* 2017, Griscom *et al* 2017).

The future of the current forest C sink is dependent both upon forest responses to climate change and human land use decisions, with land use change itself strongly influencing the course of climate change (Friedlingstein *et al* 2006). Regrowing forests (i.e., secondary forests) will play a particularly important role (Pugh *et al* 2019), as almost two-thirds of the world's forests were secondary as of 2010 (FAO 2010). As anthropogenic and climate-driven disturbances impact a growing proportion of Earth's forests (Andela *et al* 2017, McDowell *et al* 2020), understanding the carbon dynamics of regrowth forests is increasingly important (Anderson-Teixeira *et al* 2013). Although age trends in aboveground biomass have been well-studied and synthesized globally (Cook-Patton *et al* 2020), there is a relative dearth of data and synthesis on other C stocks and fluxes in secondary forests. Understanding age-related trends in forest C cycling is particularly critical for reducing uncertainty regarding the potential for carbon uptake and climate change mitigation by regrowth forests (Krause *et al* 2018, Cook-Patton *et al* 2020).

Evolution of forest C cycle research

For more than half a century, researchers have sought to understand how forest carbon cycling varies across stands, including among biomes (e.g., Lieth 1973, Luyssaert *et al* 2007) and with stand age (e.g., Odum 1969, Luyssaert *et al* 2008). Over this time, an increasingly refined conceptual understanding of the elements of ecosystem C cycles has developed, as a growing number of variables have been defined, along with appropriate measurement methods (e.g., Clark *et al* 2001, Chapin *et al* 2006). New technology has also enabled researchers to directly measure an expanding set of variables, notably including continuous measurements of soil CO_2 efflux (Kuzyakov 2006) and ecosystem-atmosphere CO_2 exchange (Baldocchi *et al* 2001). Measurement techniques have been increasingly standardized, such as the biomass allometries that strongly influence estimates of most C cycle variables (e.g., Chave *et al* 2014). Further standardization has been made possible through research networks such as ForestGEO (Anderson-Teixeira *et al* 2015, Davies *et al* 2021), NEON (Schimel *et al* 2007), and FLUXNET (Baldocchi *et al* 2001, Novick *et al* 2018). Remote sensing technology has become increasingly useful for global- or regional-scale estimates of a few critical variables, including aboveground biomass (B_{ag}, Saatchi *et al* 2011, Hu *et al* 2016, Spawn *et al* 2020) and GPP (Li and Xiao 2019). Yet, measurement and validation of most forest C stocks and fluxes requires intensive on-the-ground data collection.

Alongside these conceptual and methodological developments, there has been a proliferation of measurements across the world's forests. The result of decades of research on forest C cycling is tens of thousands of records distributed across thousands of scientific articles, varying in data formats, units, measurement methods, etc. To address questions at a global scale, researchers began synthesizing data into increasingly large databases (e.g., Lieth 1973, Luyssaert *et al* 2007, Bond-Lamberty and Thomson 2010, Anderson-Teixeira *et al* 2016, 2018, Cook-Patton *et al* 2020). The current largest, most comprehensive database on forest C cycling is *ForC* (Anderson-Teixeira *et al* 2016, 2018), which contains published estimates of forest ecosystem C stocks and annual fluxes (>50 variables), with different variables capturing distinct ecosystem pools (e.g., woody, foliage, and root biomass; dead wood) and flux types (e.g, gross and net primary productivity; soil, root, and ecosystem respiration). These data represent ground-based measurements, and *ForC* contains associated data required for interpretation (e.g., stand history, measurement methods). Since its most recent publication (*ForC v2.0-Ecology*, Anderson-Teixeira *et al* 2018), *ForC* has grown 129%, primarily through the incorporation of two additional large databases that also synthesized published forest C data: the Global Soil Respiration Database (SRDB, Bond-Lamberty and Thomson 2010, Jian *et al* 2020) and the Global Reforestation Opportunity Assessment database (GROA, Cook-Patton *et al* 2020). Following these additions, *ForC* currently contains 39762 records from 10608 plots and 1532 distinct geographic areas representing all forested biogeographic and climate zones, making it ideal for assessing how forest C cycling varies across biomes and with respect to stand age.

Biome differences

Forest C cycling varies enormously across biomes, categories that encapsulate major differences in climate and vegetation. The dominant role of climate in shaping global variation among forests has been recognized since the early 19$^{\text{th}}$ century (Humboldt and Bonpland 1807, Holdridge 1947). Global scale data syntheses have shown that C fluxes including GPP, net primary productivity (NPP), and soil respiration (R_{soil}) decrease with latitude or, correspondingly, increase with mean annual temperature (Fig. 1a; e.g., Lieth 1973, Luyssaert *et al* 2007, Hursh *et al* 2017, Banbury Morgan *et al* in press). C stocks of mature forests show less directional variation (Fig. 1c). On average, aboveground biomass (B_{ag}) tends to decrease with latitude, but not as dramatically as fluxes, and with the highest biomass forests in relatively cool, moist temperate regions (Smithwick *et al* 2002, Keith *et al* 2009, Hu *et al* 2016). In contrast, standing and downed dead wood ($DW_{standing}$ and DW_{down}, respectively, summing to DW_{tot}) and the organic layer (OL) tend to accumulate more in colder climates where decomposition is slow relative to NPP (Harmon *et al* 1986, Allen *et al* 2002).

Phenomenological analyses relating C stocks and fluxes to climate and other environmental variables have recently been taken to a new level through use of machine-learning algorithms that relate ground-based C cycle data to global maps of environmental covariates (e.g., Warner *et al* 2019, Cook-Patton *et al* 2020). The resulting models enable construction of fine-scale global maps of estimated C cycling variables. This approach can be particularly effective when it integrates satellite measurements that correlate with C cycle variables of interest; for example, solar-induced chlorophyll fluorescence is useful for fine-scale mapping of gross primary productivity (GPP, Li and Xiao 2019), while LiDAR, radar, and optical imagery are being used to model B_{ag} at regional to global scales (e.g., Saatchi *et al* 2011, Hu *et al* 2016). However, all such analyses are ultimately constrained by the quality and coverage of ground-based estimates of forest C fluxes or stocks to train models (e.g., Schepaschenko *et al* 2019). While estimates of some variables (e.g., B_{ag}, GPP, NPP, R_{soil}) are widely available, many remain poorly characterized (e.g., DW_{tot}; OL; autotrophic respiration, R_{auto}), even at the coarse resolution of biomes. This is a critical limitation for understanding forest C cycling and quantifying forest-based climate change mitigation potential across forest biomes or ecozones (e.g., IPCC 2019).

Age trends and their variation across biomes

Stand age is another important axis of variation in forest C cycling (Fig. 1b,d). In 1969, E.P. Odum's "The Strategy of Ecosystem Development" laid out predictions as to how forest energy flows and organic matter stocks vary with stand age (Odum 1969). Although the conceptualization of the C cycle in this paper was simplistic by current standards, the paper was foundational in framing the theory around which research on the subject still revolves (Corman *et al* 2019), and the basic framework still holds, albeit with modest modifications (Fig. 1b, Anderson-Teixeira *et al* 2013). Following stand-clearing disturbance, GPP, NPP, and biomass of leaves ($B_{foliage}$) and fine roots ($B_{root-fine}$) initially increase rapidly and thereafter remain relatively stable ($B_{foliage}$, $B_{root-fine}$, sometimes GPP) or decline slightly (NPP, sometimes GPP; e.g., Law *et al* 2003, Pregitzer and Euskirchen 2004, Amiro *et al* 2010, Goulden *et al* 2011). The decline in NPP occurs because R_{auto} increases relative to GPP as forests age, corresponding to declining carbon use efficiency with stand age (DeLucia *et al* 2007, Collalti *et al* 2020). Heterotrophic respiration, most of which originates from the soil ($R_{het-soil}$), remains relatively constant with stand age (Law *et al* 2003, Pregitzer and Euskirchen 2004, Goulden *et al* 2011). As a result, net ecosystem production ($NEP = GPP - R_{eco}$, where R_{eco} is total ecosystem respiration) is initially negative, increases to a maximum at intermediate ages, and thereafter declines – typically to a small positive value (Law *et al* 2003, Pregitzer and Euskirchen 2004, Luyssaert *et al* 2008, Amiro *et al* 2010, Goulden *et al* 2011). The result is that biomass accumulation is rapid in young forests, followed by a slow decline to near zero in old forests (e.g., Lichstein *et al* 2009, Yang *et al* 2011). While these trends have been the subject of fairly recent qualitative review (Anderson-Teixeira *et al* 2013), there is need for a synthetic, quantitative review taking advantage of the greatly expanded data now available.

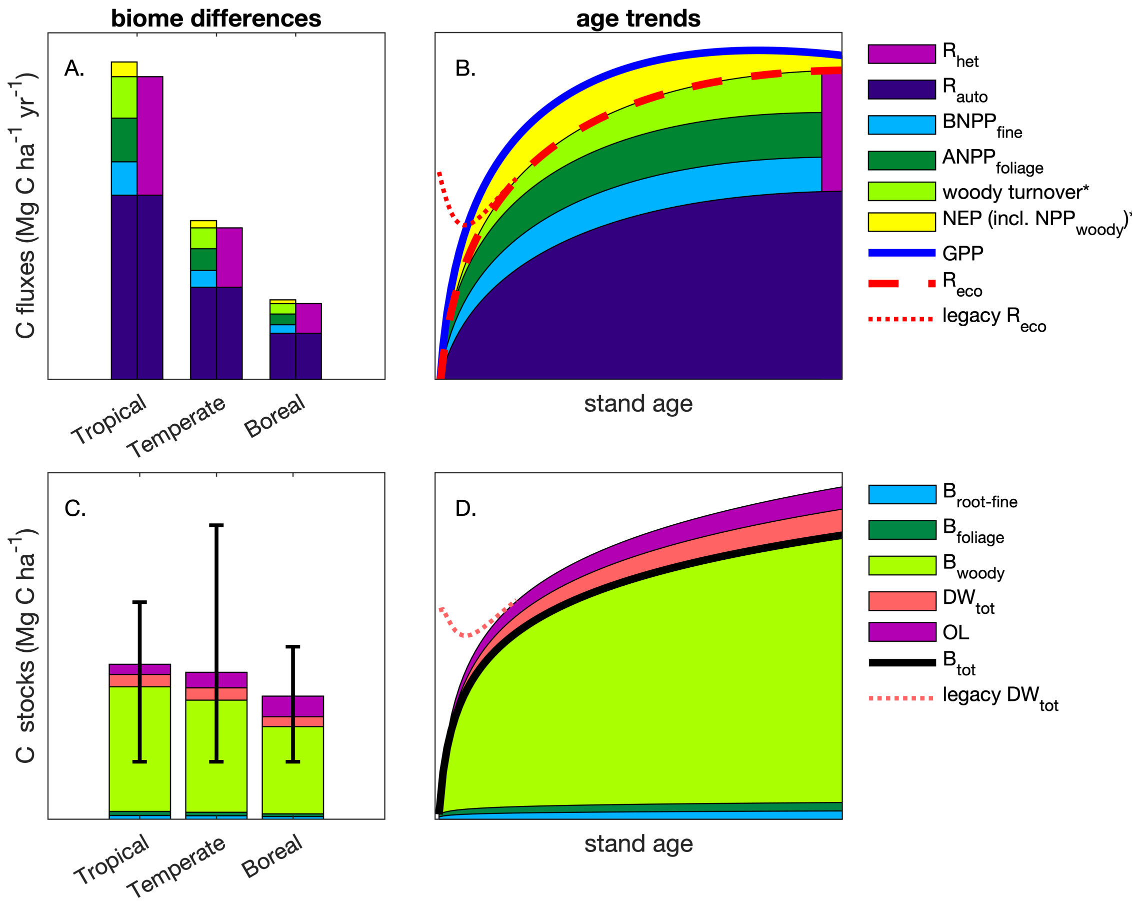

Figure 1 | Schematic diagram summarizing current understanding of biome differences (a,c) and age trends (b,d) in forest C cycling. Variables are defined in Table 1. Age trends, which represent idealized dynamics following a disturbance that removes all living vegetation, are an updated version of the classic figure from Odum (1969), with heavy lines (b,d) corresponding to those in Odum's figure 1 and NEP corresponding to Odum's 'net production' (b). *Positive NEP of young forests is typically dominated by woody NPP ($NPP_{woody} = ANPP_{woody} + BNPP_{coarse}$). As forests age and biomass accumulation slows, NPP_{woody} approaches equilibrium with woody turnover (M_{woody} + $ANPP_{branch}$ + coarse root turnover), and NEP may be dominated by changes in dead wood or soil organic carbon. Dotted lines refer to decomposition of potential 'legacy' organic material produced prior to the disturbance and remaining at the site (e.g., standing and fallen dead wood, DW_{tot}; soil organic matter). Error bars on C stocks plot represent within-biome variability, wherein mean biomass is highest in the tropics, but maximum biomass is highest in temperate regions.

In the past few decades, researchers have started asking how age trends – mostly in B_{ag} or total biomass (B_{tot}) accumulation – vary across biomes. Early research on this theme showed that biomass accumulation rates during secondary succession increase with temperature on a global scale (Johnson *et al* 2000, Anderson *et al* 2006) and with water availability in the neotropics (Poorter *et al* 2016). Cook-Patton *et al* (2020) reinforced these earlier findings with a much larger dataset and created a high-resolution global map of estimated potential C accumulation rates. However, there has been little synthesis of cross-biome differences in variables other than biomass and its accumulation rate (but see Cook-Patton *et al* 2020 for DW, OL, and soil C accumulation in young stands). Given the important role of secondary forests in the current and future global C cycle, a concrete understanding of age trends in C fluxes and stocks and how these vary across biomes is critical to better understanding the global C cycle. Accurate estimates of C sequestration rates by regrowth forests are also critical for national greenhouse gas accounting under the IPCC framework

(IPCC 2019, Requena Suarez *et al* 2019) and quantifying the value of regrowth forests for climate change mitigation (Anderson-Teixeira and DeLucia 2011, Goldstein *et al* 2020).

Here, we conduct a data-based review of carbon cycling from a stand to global level, and by biome and stand age, using our open-source Global Carbon Forest database (*ForC*; Fig. 2). Our goal is to provide a comprehensive synthesis on broad trends in forest C cycling that can serve as a foundation for improved understanding of global forest C cycling and highlight where key sources of uncertainty still reside.

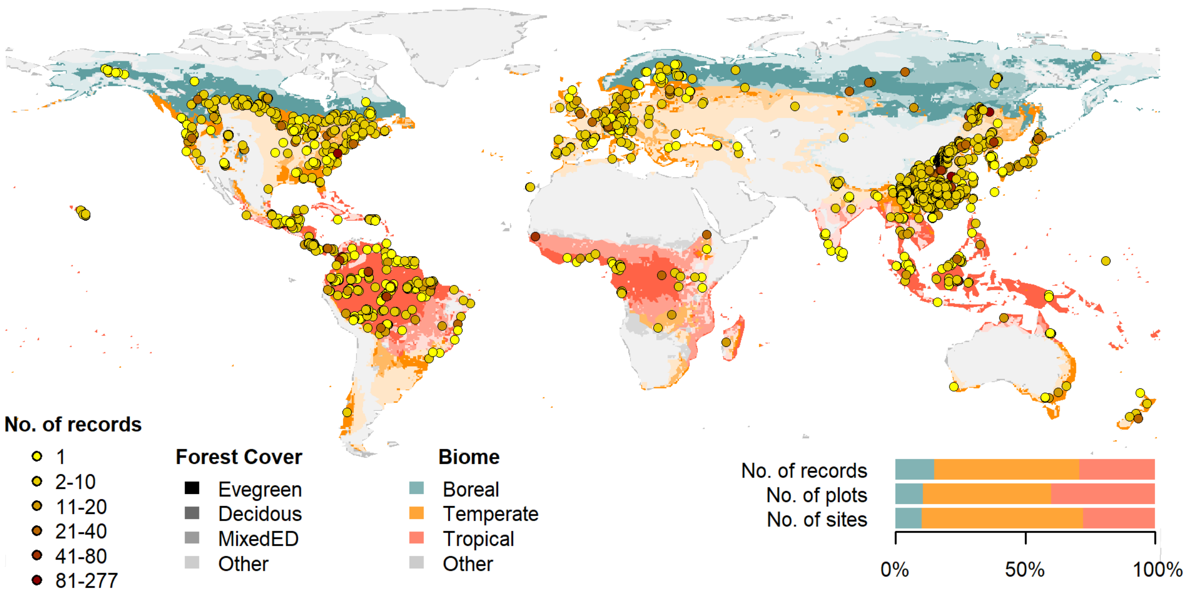

Figure 2 | Map of sites included in this analysis. Symbols are colored according to the number of records at each site. Underlying map shows coverage of evergreen, deciduous, and mixed forests (shading differences; data from Jung et al. 2006) and biomes (color differences). Distribution of sites, plots, and records among biomes is shown in the inset.

Methods/ Design

This review synthesizes data from the *ForC* database (Fig. 2, https://github.com/forc-db/ForC, Anderson-Teixeira *et al* 2016, 2018). *ForC* amalgamates numerous intermediary data sets (e.g., Luyssaert *et al* 2007, Bond-Lamberty and Thomson 2010, Cook-Patton *et al* 2020) and original studies. Original publications were referenced to check values and obtain information not contained in intermediary data sets, although this process has not been completed for all records. The database was developed with goals of understanding how C cycling in forests varies across broad geographic scales and as a function of stand age. As such, there has been a focus on incorporating data from regrowth forests (e.g., Anderson *et al* 2006, Martin *et al* 2013, Bonner *et al* 2013) and obtaining stand age data when possible (83% of records in *ForC* v.2.0, Anderson-Teixeira *et al* 2018). Particular attention was given to developing the database for tropical forests (Anderson-Teixeira *et al* 2016), which represented roughly one-third of records in *ForC* v2.0 (Anderson-Teixeira *et al* 2018). Since publication of ForC v2.0, we imported three large additional databases into *ForC* via a combination of R scripts and manual edits. First, we imported (via R script) the Global Soil

Respiration Database (*SRDB* v4, 9488 records, Bond-Lamberty and Thomson 2010), with corrections and improvements to *SRDB* arising from this process incorporated into *SRDB* v5 (Jian *et al* 2020). Second, we imported (via R script) the Global Reforestation Opportunity Assessment database (*GROA* v1.0, 10116 records, Cook-Patton *et al* 2020, Anderson-Teixeira *et al* 2020), which itself had drawn on an earlier version of *ForC*. Because all records in *GROA* were checked against original publications, these records were given priority over duplicates in *ForC* (Appendix S1). Third, we incorporated records of annual NEP, GPP, and R_{eco} from the FLUXNET2015 dataset (Pastorello *et al* 2020), treating these records as authoritative when they duplicated earlier records (Appendix S1). We have also added data from individual publications, focusing on productivity (e.g., Taylor *et al* 2017), dead wood, and ForestGEO sites (e.g., Johnson *et al* 2018, Lutz *et al* 2018). A record of data sets added to *ForC* over the course of its development is available at https://github.com/forc-db/ForC/blob/master/database_management_records/ForC_data_additions_log.csv. The database version used for this analysis has been tagged as a new release on Github (v3.0) and assigned a DOI through Zenodo (DOI: 10.5281/zenodo.4571538).

All measurements originally expressed in units of dry organic matter (OM) were converted to units of C using the IPCC default of $C = 0.47 * OM$ (IPCC 2018). Duplicate or otherwise conflicting records were purged as described in Appendix S1, resulting in a total of 22265 records (56% size of total database). Records were filtered to remove plots that had undergone significant anthropogenic management or major disturbance since the most recent stand initiation event. Specifically, we removed plots with any record of managements manipulating CO_2, temperature, hydrology, nutrients, or biota, as well as any plots whose site or plot name contained the terms "plantation," "planted," "managed," "irrigated," or "fertilized" (13.9% of duplicate-purged records). We also removed stands that had undergone any notable anthropogenic thinning or partial harvest (5.6% of duplicate-purged records). We retained sites that were grazed or had undergone low severity natural disturbances (<10% mortality) including droughts, major storms, fires, and floods. We removed all plots for which no stand history information had been retrieved (5.7% of duplicate-purged records). In total, this resulted in 17349 records (43.6% of the records in the database) being eligible for inclusion in the analysis.

We selected 23 annual flux and 11 C stock variables for inclusion in the analysis (Table 1). These different flux and stock variables represent different pools (e.g., aboveground biomass, root biomass, dead wood) and levels of combination (e.g., total net primary productivity, NPP, versus the individual elements of NPP such as foliage, roots, and branches). We did not analyze soil carbon, which is not a focus of the *ForC* database. Note that two flux variables, aboveground heterotrophic respiration (R_{het-ag}) and total heterotrophic respiration (R_{het}), were included for conceptual completeness but had no records in *ForC* (Table 1). Records for our focal variables represented 90.3% of the total records eligible for inclusion. For this analysis, we combined some specific variables from *ForC* into more broadly defined variables. Specifically, net ecosystem exchange (measured by eddy-covariance, Baldocchi *et al* 2001) and biometric estimates of NEP were combined into the single variable NEP (Table 1). Furthermore, for NPP, aboveground NPP ($ANPP$), and the litterfall component of $ANPP$ ($ANPP_{litterfall}$), we combined ForC variables specifying inclusion or exclusion of minor components (e.g., measurements including or excluding fruit production, flower production, and herbivory). Throughout ForC, for all measurements drawing from tree census data (e.g., biomass, productivity), trees were censused down to a minimum diameter breast height (DBH) threshold of 10 cm or less. All records were based on ground-based field measurements.

We grouped forests into four broad biome types (tropical broadleaf, temperate broadleaf, temperate

Table 1. Carbon cycle variables included in this analysis, their sample sizes, and summary of biome differences and age trends.

Variable	Description	N records			biome differences*	age trend†
		records	plots	geographic areas		
Annual fluxes						
NEP	net ecosystem production or net ecosystem exchange (+ indicates C sink)	329	146	88	n.s.	+; xB
GPP	gross primary production ($NPP + R_{auto}$ or $NEP + R_{eco}$)	303	115	84	TrB > TeB ≥ TeN ≥ BoN	+; xB
NPP	net primary production ($ANPP$ + $BNPP$)	214	112	74	TrB > TeB ≥ TeN > BoN	n.s.
$ANPP$	aboveground NPP	343	236	131	TrB > TeB ≥ TeN > BoN	+; xB
$ANPP_{woody}$	woody production ($ANPP_{stem}$ + $ANPP_{branch}$)	64	53	37	n.s.	+
$ANPP_{stem}$	woody stem production	217	190	117	TrB > TeN ≥ TeB ≥ BoN	n.s.
$ANPP_{branch}$	branch turnover	69	59	42	TrB > TeB ≥ TeN	n.s.
$ANPP_{foliage}$	foliage production, typically estimated as annual leaf litterfall	162	132	88	TrB > TeB ≥ TeN > BoN	+
$ANPP_{litterfall}$	litterfall, including leaves, reproductive structures, twigs, and sometimes branches	82	70	55	n.s.	+
$ANPP_{repro}$	production of reproductive structures (flowers, fruits, seeds)	51	44	34	n.t.	n.t.
$ANPP_{folivory}$	foliar biomass consumed by folivores	20	12	11	n.t.	n.t.
M_{woody}	woody mortality–i.e., B_{ag} of trees that die	18	18	18	n.t.	n.t.
$BNPP$	belowground NPP ($BNPP_{coarse}$+ $BNPP_{fine}$)	148	116	79	TrB > TeN ≥ TeB ≥ BoN	+
$BNPP_{coarse}$	coarse root production	77	56	36	TeN ≥ TrB	n.s.
$BNPP_{fine}$	fine root production	123	99	66	n.s.	+
R_{eco}	ecosystem respiration (R_{auto}+ R_{het})	213	98	70	TrB > TeB ≥ TeN	+
R_{auto}	autotrophic respiration ($R_{auto-ag} + R_{root}$)	24	23	15	n.t.	n.t.
$R_{auto-ag}$	aboveground autotrophic respiration (i.e., leaves and stems)	2	2	1	n.t.	n.t.
R_{root}	root respiration	181	139	95	TrB ≥ TeB	+
R_{soil}	soil respiration ($R_{het-soil} + R_{root}$)	627	411	229	TrB > TeB > TeN ≥ BoN	n.s.
$R_{het-soil}$	soil heterotrophic respiration	197	156	100	TrB > TeB ≥ TeN	n.s.
R_{het-ag}	aboveground heterotrophic respiration	0	0	0	-	-
R_{het}	heterotrophic respiration ($R_{het-ag} + R_{het-soil}$)	0	0	0	-	-
Stocks						
B_{tot}	total live biomass (B_{ag}+B_{root})	188	157	87	TrB ≥ TeB > BoN	+; xB
B_{ag}	aboveground live biomass ($B_{ag-wood}$+$B_{foliage}$)	4466	4072	621	TrB ≥ TeN ≥ TeB > BoN	+; xB
$B_{ag-wood}$	woody component of aboveground biomass	115	102	64	TeN > TrB ≥ BoN	+; xB
$B_{foliage}$	foliage biomass	134	115	72	TeN > TrB ≥ BoN ≥ TeB	+; xB
B_{root}	total root biomass ($B_{root-coarse}$+$B_{root-fine}$)	2329	2298	360	n.s.	+; xB
$B_{root-coarse}$	coarse root biomass	134	120	73	TeN > TeB ≥ BoN	+; xB
$B_{root-fine}$	fine root biomass	226	180	109	n.s.	+; xB
DW_{tot}	deadwood ($DW_{standing}$+DW_{down})	79	73	42	n.t.	+; xB
$DW_{standing}$	standing dead wood	36	35	22	n.t.	n.t.
DW_{down}	fallen dead wood, including coarse and sometimes fine woody debris	278	265	37	n.t.	+; xB
OL	organic layer / litter/ forest floor	474	413	115	n.s.	+; xB

* TrB: Tropical, TeB: Temperate Broadleaf, TeN: Temperate Needleleaf, BoN: Boreal, n.s.: no significant differences, n.t.: not tested

† + or -: significant positive or negative trend, xB: significant age x biome interaction, n.s.: no significant age trend, n.t.: not tested

needleleaf, and boreal needleleaf) and two age classifications (young and mature). The climate component of the biome definitions (Fig. 2) was based on site geographic coordinates according to Köppen-Geiger zones

(Rubel and Kottek 2010). We defined the tropical biome as including all equatorial (A) zones, temperate biomes as including all warm temperate (C) zones and warmer snow climates (Dsa, Dsb, Dwa, Dwb, Dfa, and Dfb), and the boreal biome as including the colder snow climates (Dsc, Dsd, Dwc, Dwd, Dfc, and Dfd). Forests in dry (B) and polar (E) Köppen-Geiger zones were excluded from the analysis. We distinguished broadleaf and needleleaf forests based on descriptions in original publications (prioritized) or values extracted from a global map based on satellite observations (SYNMAP, Jung *et al* 2006). For young tropical forests imported from *GROA* but not yet classified by leaf type, we assumed that all were broadleaf, consistent with the rarity of naturally regenerating needleleaf forests in the tropics. We classified forests as "young" if stand age was less than 100 years, or "mature" if stand age was older or if they were described as "mature," "old growth," "intact," or "undisturbed" in the original publication. Assigning stands to these groupings required excluding records for which *ForC* lacked geographic coordinates (0.4% of sites in the full database) or records of stand age or forest maturity (5.7% of records in the full database). We also excluded records with stand age of zero years (0.8% of records in full database). In total, our analysis retained 11923 records. Numbers of records by biome and age class are provided in Table S1.

We calculated the means and standard deviations of each mature forest C cycle variable by biome over geographically distinct areas to produce biome-specific schematics. We first averaged any repeated measurements within a plot. To avoid pseudo-replication, we then averaged multiple measurements within geographically distinct areas, defined as plots clustered within 25 km of one another (*sensu* Anderson-Teixeira *et al* 2018), weighting by area sampled if available for all records. Finally, we took means and standard deviations over geographic areas.

We tested whether the C budgets described above "closed"–*i.e.*, whether they were internally consistent. Specifically, we first defined relationships among variables (e.g., $NEP = GPP - R_{eco}$, $BNPP = BNPP_{coarse} + BNPP_{fine}$, $DW_{tot} = DW_{standing} + DW_{down}$). Henceforth, we refer to the variables on the left side of the equation as "aggregate" fluxes or stocks, and those that are summed as "component" fluxes or stocks, noting that the same variable can take both aggregate and component positions in different relationships. We considered the C budget for a given relationship "closed" when the means of component variables summed to within one standard deviation of the mean of the aggregate variable.

To test for differences across mature forest biomes, we also examined how stand age impacted fluxes and stocks, employing a mixed effects model ('lmer' function in 'lme4' R package, Bates *et al* 2015) with biome as a fixed effect and plot nested within geographic area as random effects on the intercept. When biome had a significant effect, we used Tukey's pairwise comparison to see which biomes were significantly different from one another. This analysis was run for variables and biomes with records for at least seven distinct geographic areas per biome (Table 1).

To test for age trends in young (<100yrs) forests, we employed a mixed effects model with biome and log10[stand age] as fixed effects and plot nested within geographic area as a random effect on the intercept. This analysis was run for variables and biomes with records for at least three distinct geographic areas per biome, excluding any biomes that failed this criterion (Table 1). When the effect of stand age was significant at $p \leq 0.05$, and when each biome had records for stands of at least ten different ages, a biome × stand age interaction was included in the model. We note that the logarithmic function fit in this analysis does not always correspond to theoretical expectations, particularly for NEP (Fig. 1b); however, data limitations did not support fitting of functions with more parameters or reliable comparisons of different functional forms. Within the data constraints, we deemed a logarithmic function to be the appropriate functional form for most variables.

To facilitate the accessibility of our results and data, and to allow for rapid updates as additional data become available, we automated all database manipulation, analyses, and figure production in R (Team 2020).

Review Results/ Synthesis

Data Coverage

Of the 39762 records in *ForC* v3.0, 11923 met our strict criteria for inclusion in this study (Fig. 2). These records were distributed across 5062 plots in 865 distinct geographic areas. Of the 23 flux and 11 stock variables mapped in our C cycle diagrams (Figs. 3-6, S1-S4), *ForC* contained sufficient mature forest data for inclusion in our statistical analyses (*i.e.*, records from ≥ 7 distinct geographic areas) for 20 fluxes and 9 stocks in tropical broadleaf forests, 15 fluxes and 8 stocks in temperate broadleaf forests, 14 fluxes and 7 stocks in temperate conifer forests, and 8 fluxes and 7 stocks in boreal forests. For regrowth forests (<100 yrs), *ForC* contained sufficient data for inclusion in our statistical analyses (*i.e.*, records from ≥ 3 distinct geographic areas) for 11 fluxes and 10 stocks in tropical broadleaf forests, 16 fluxes and 10 stocks in temperate broadleaf forests, 16 fluxes and 10 stocks in temperate conifer forests, and 14 fluxes and 9 stocks in boreal forests.

C cycling in mature forests

Average C cycles for mature tropical broadleaf, temperate broadleaf, temperate conifer, and boreal forests are presented in Figures 3-6 (and available in tabular format in the *ForC* release accompanying this publication: `ForC/numbers_and_facts/ForC_variable_averages_per_Biome.csv`).

For variables with records from ≥ 7 distinct geographic areas, these ensemble C budgets met our criteria for budget "closure." That is, component variables summed to within one standard deviation of their respective aggregate variables in all but one instance. In the temperate conifer biome, the average composite measure of root biomass (B_{root}) was less than the combined average value of coarse and fine root biomass ($B_{root-coarse}$ and $B_{root-fine}$, respectively). This lack of closure was driven by very high estimates of $B_{root-coarse}$ from high-biomass forests of the US Pacific Northwest, a geographic region with a disproportionately large number of records for this variable (Fig. S25).

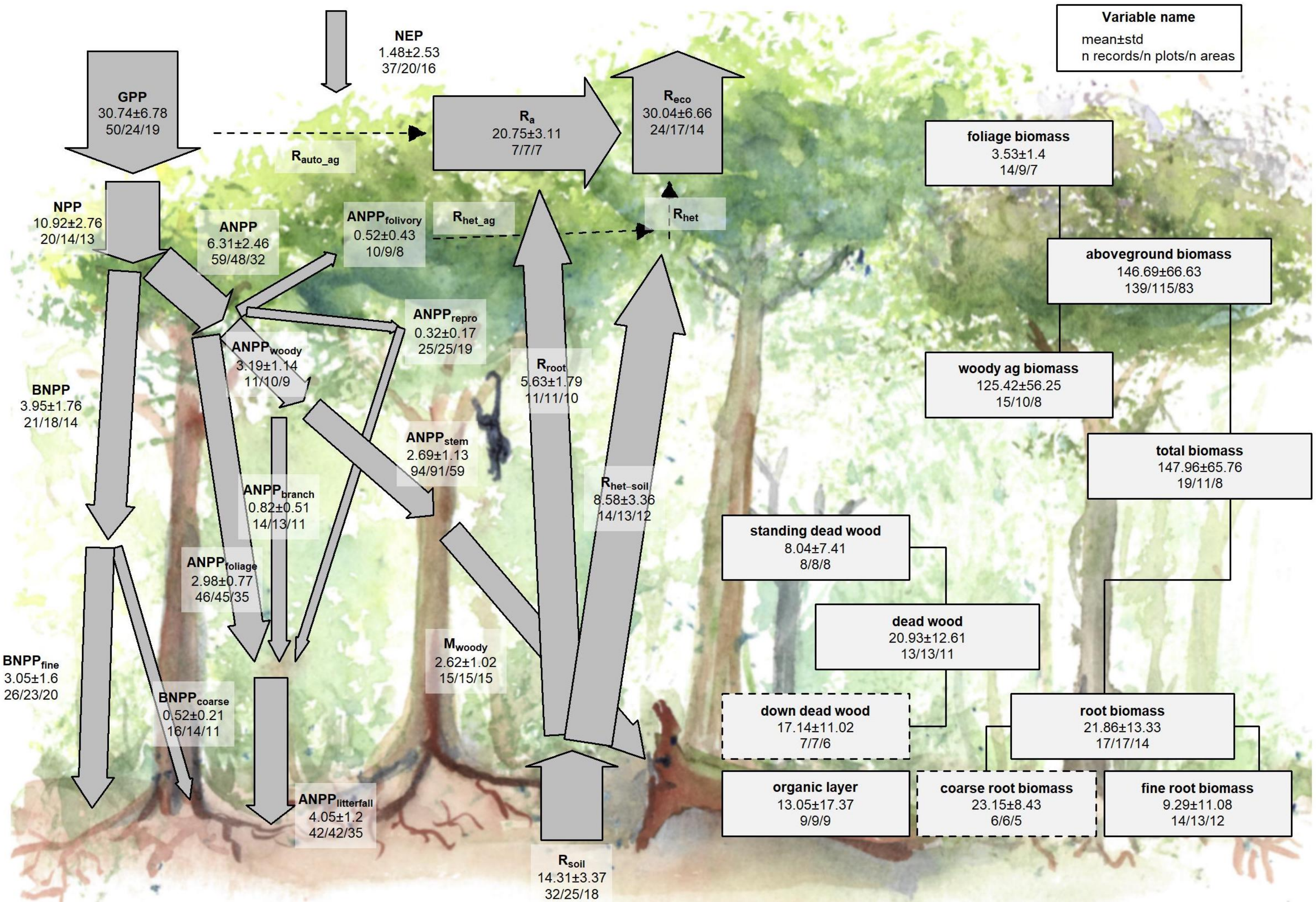

Figure 3 | C cycle diagram for mature tropical broadleaf forests. Arrows indicate fluxes (Mg C ha^{-1} yr^{-1}); boxes indicate stocks (Mg C ha^{-1}), with variables as defined in Table 1. Presented are mean ± std over geographically distinct areas (clusters of plots within 25 km of each other). Dashed shape outlines indicate variables with records from <7 distinct geographic areas, and dashed arrows indicate fluxes with no data. To illustrate the magnitude of different fluxes, arrow width is proportional to the square root of the corresponding flux. Mean component fluxes do not necessarily add up to the mean total fluxes because different sets of sites are included depending on data availability (Figs. S5-S30). Mature forests are defined as ≥ 100 years old and with no known major natural or anthropogenic disturbance in that time.

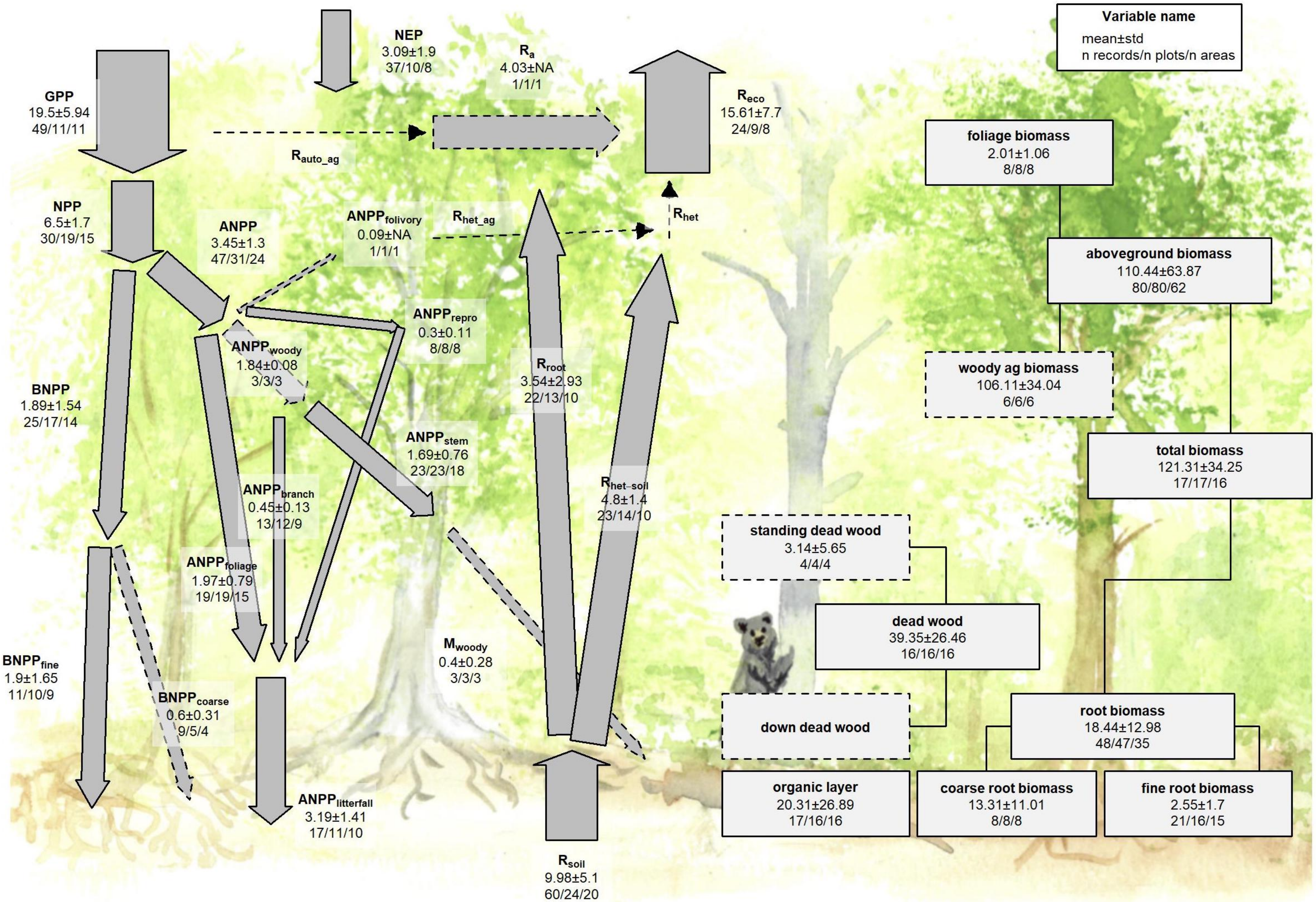

Figure 4 | C cycle diagram for mature temperate broadleaf forests. Arrows indicate fluxes (Mg C ha^{-1} yr^{-1}); boxes indicate stocks (Mg C ha^{-1}), with variables as defined in Table 1. Presented are mean ± std over geographically distinct areas (clusters of plots within 25 km of each other). Dashed shape outlines indicate variables with records from <7 distinct geographic areas, and dashed arrows indicate fluxes with no data. To illustrate the magnitude of different fluxes, arrow width is proportional to the square root of the corresponding flux. Mean component fluxes do not necessarily add up to the mean total fluxes because different sets of sites are included depending on data availability (Figs. S5-S30). Mature forests are defined as $\geq$ 100 years old and with no known major natural or anthropogenic disturbance in that time.

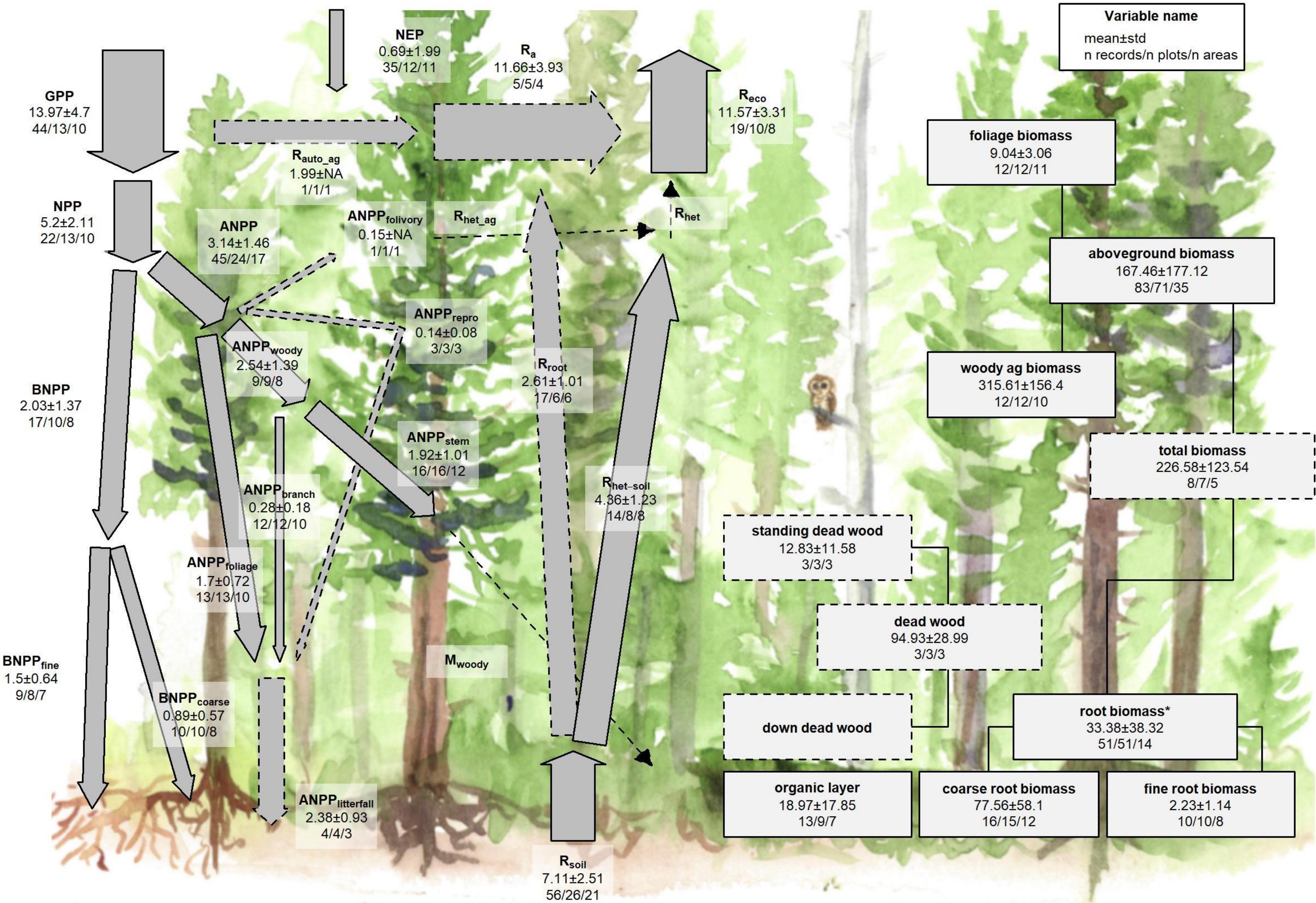

Figure 5 | C cycle diagram for mature temperate conifer forests. Arrows indicate fluxes (Mg C ha^{-1} yr^{-1}); boxes indicate stocks (Mg C ha^{-1}), with variables as defined in Table 1. Presented are mean ± std over geographically distinct areas (clusters of plots within 25 km of each other). Dashed shape outlines indicate variables with records from <7 distinct geographic areas, and dashed arrows indicate fluxes with no data. To illustrate the magnitude of different fluxes, arrow width is proportional to the square root of the corresponding flux. Mean component fluxes do not necessarily add up to the mean total fluxes because different sets of sites are included depending on data availability (Figs. S5-S30). Mature forests are defined as ≥ 100 years old and with no known major natural or anthropogenic disturbance in that time. The temperate conifer biome in particular is subject to high variability, with highest fluxes and stocks in the high-biomass forests of the US Pacific Northwest. An asterisk after a variable name indicates lack of C cycle closure.

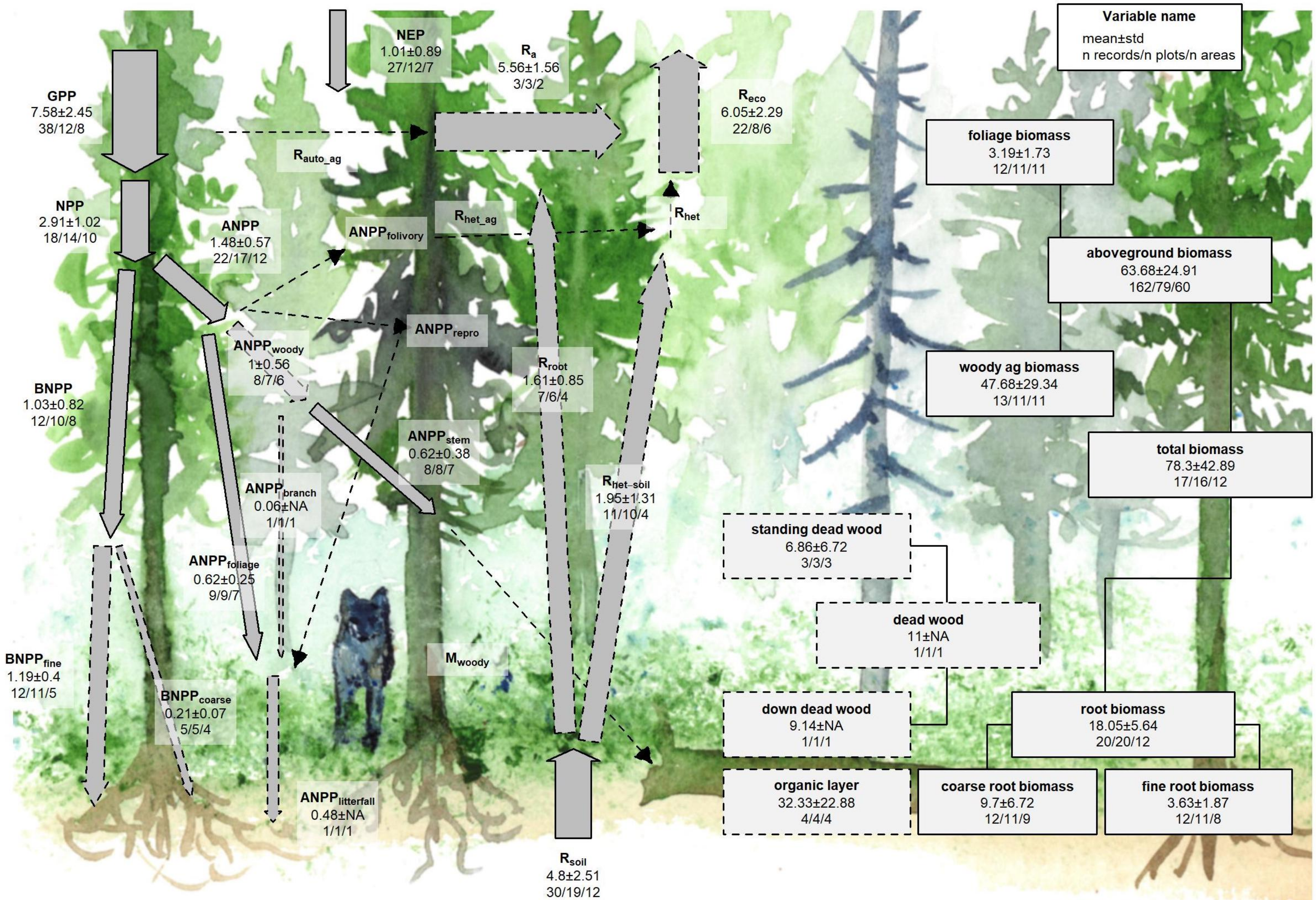

Figure 6 | C cycle diagram for mature boreal conifer forests. Arrows indicate fluxes (Mg C ha^{-1} yr^{-1}); boxes indicate stocks (Mg C ha^{-1}), with variables as defined in Table 1. Presented are mean ± std over geographically distinct areas (clusters of plots within 25 km of each other). Dashed shape outlines indicate variables with records from <7 distinct geographic areas, and dashed arrows indicate fluxes with no data. To illustrate the magnitude of different fluxes, arrow width is proportional to the square root of the corresponding flux. Mean component fluxes do not necessarily add up to the mean total fluxes because different sets of sites are included depending on data availability (Figs. S5-S30). Mature forests are defined as ≥ 100 years old and with no known major natural or anthropogenic disturbance in that time.

There were sufficient data to assess differences among biomes in mature forest values for 15 flux variables, and 12 of these variables exhibited statistically significant differences among biomes (Table 1). In all cases of significant differences (including C fluxes into, within, and out of the ecosystem), C fluxes were highest in tropical forests, intermediate in temperate (broadleaf or conifer) forests, and lowest in boreal forests (Table 1, Figs. 7, S5-S19). Differences between tropical and boreal forests were consistently significant, with temperate forests intermediate and significantly different from one or both. Fluxes tended to be numerically greater in temperate broadleaf than temperate conifer forests, but the difference was never statistically significant. This pattern held for 11 of the 12 variables with significant biome effects: GPP, NPP, $ANPP$, $ANPP_{stem}$,$ANPP_{branch}$, $ANPP_{foliage}$, $BNPP$, R_{eco}, R_{root}, R_{soil}, and $R_{het-soil}$. For two of the variables without significant differences among biomes ($ANPP_{litterfall}$ and $BNPP_{fine}$; Figs. S12 and S15, respectively), the same general trends applied but were not statistically significant.

The most notable exception to the pattern of decreasing flux per unit area from tropical to boreal biomes was NEP, with no significant differences across biomes but with the largest average in temperate broadleaf forests, followed by tropical, boreal, and temperate conifer forests (Figs. 7, S5). For all biomes, NEP was positive, with 95% confidence intervals excluding zero. $BNPP_{root-coarse}$ also exhibited significant differences among biomes with the highest means outside the tropics, in this case in temperate conifer forest, a biome for which all records came from high-biomass forests in the US Pacific Northwest (Fig. S14; differences significant in mixed effects model but not in post-hoc pairwise comparison).

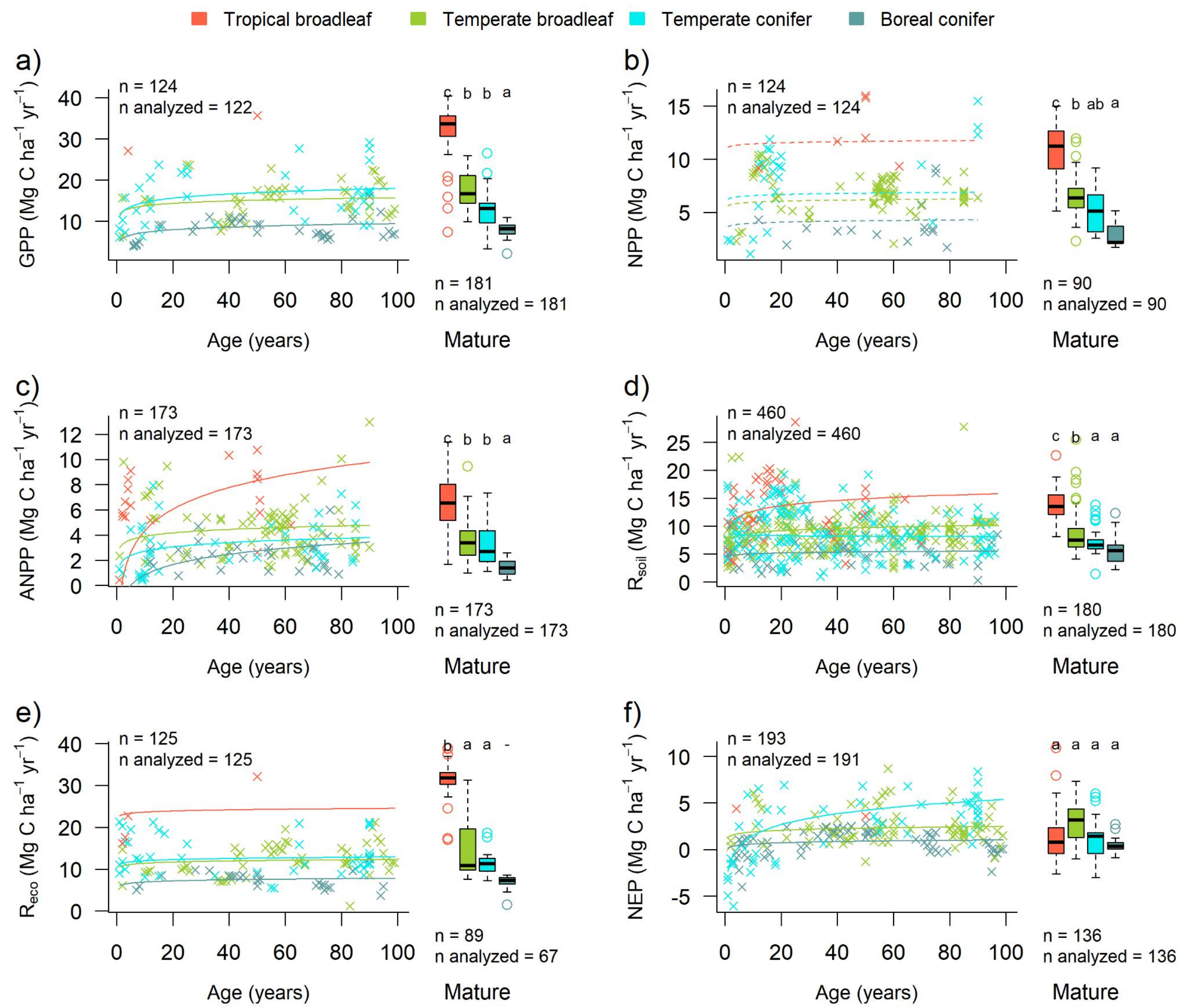

Figure 7 | Age trends and biome differences in some of the major C fluxes: (a) GPP, (b) NPP, (c) $ANPP$, (d) R_{soil}, (e) R_{eco}, and (f) NEP. The scatterplots show age trends in forests up to 100 years old, as characterized by a linear mixed effects model with fixed effects of log10(age) and biome. The fitted lines indicate the effect of age (solid lines: significant at p<0.05, dashed lines: non-significant), and non-parallel lines indicate a significant log10(age) x biome interaction (interaction effects were tested only if the main age effect was significant and data were available for at least ten stand ages per biome–i.e., for GPP, $ANPP$, R_{soil}, and NEP). The boxplots illustrate variation among biomes in mature forests, with different letters indicating significant differences between biomes. Data from biomes that did not meet the sample size criteria (see Methods) are plotted, but lack regression lines (young forests) or tests of differences across biomes (mature forests, indicated by a dash instead of a letter above the box plot). Individual figures for each flux with sufficient data, along with maps showing geographic distribution of the data, are given in the Supplement (Figs. S5-S19).

Biome differences were less consistent across C stocks than fluxes (Figs. 8, S20-S30). There were sufficient data to assess mature forest biome differences for nine stock variables, and significant differences among biomes were detected for five variables (B_{tot}, B_{ag}, $B_{ag-wood}$, $B_{foliage}$, $B_{root-coarse}$; Table 1). For B_{tot} and B_{ag}, tropical broadleaf forests had the highest mean biomass and boreal forests the lowest, with intermediate means for temperate broadleaf and needleleaf forests (temperate needleleaf excluded from B_{tot} analysis because of insufficient data; Figs. S20, S21). However, maximum values for these variables – along with all other stocks including live or standing woody biomass ($B_{ag-wood}$, B_{root}, $B_{root-coarse}$, DW_{tot}, $DW_{standing}$) – consistently occurred in temperate biomes (Figs. 1c, 8, S20-S30). For variables for which temperate conifer forest records were disproportionately from high-biomass forests in the US Pacific Northwest ($B_{ag-wood}$, $B_{foliage}$, and $B_{root-coarse}$), temperate conifer forests had significantly higher stocks than other biomes.

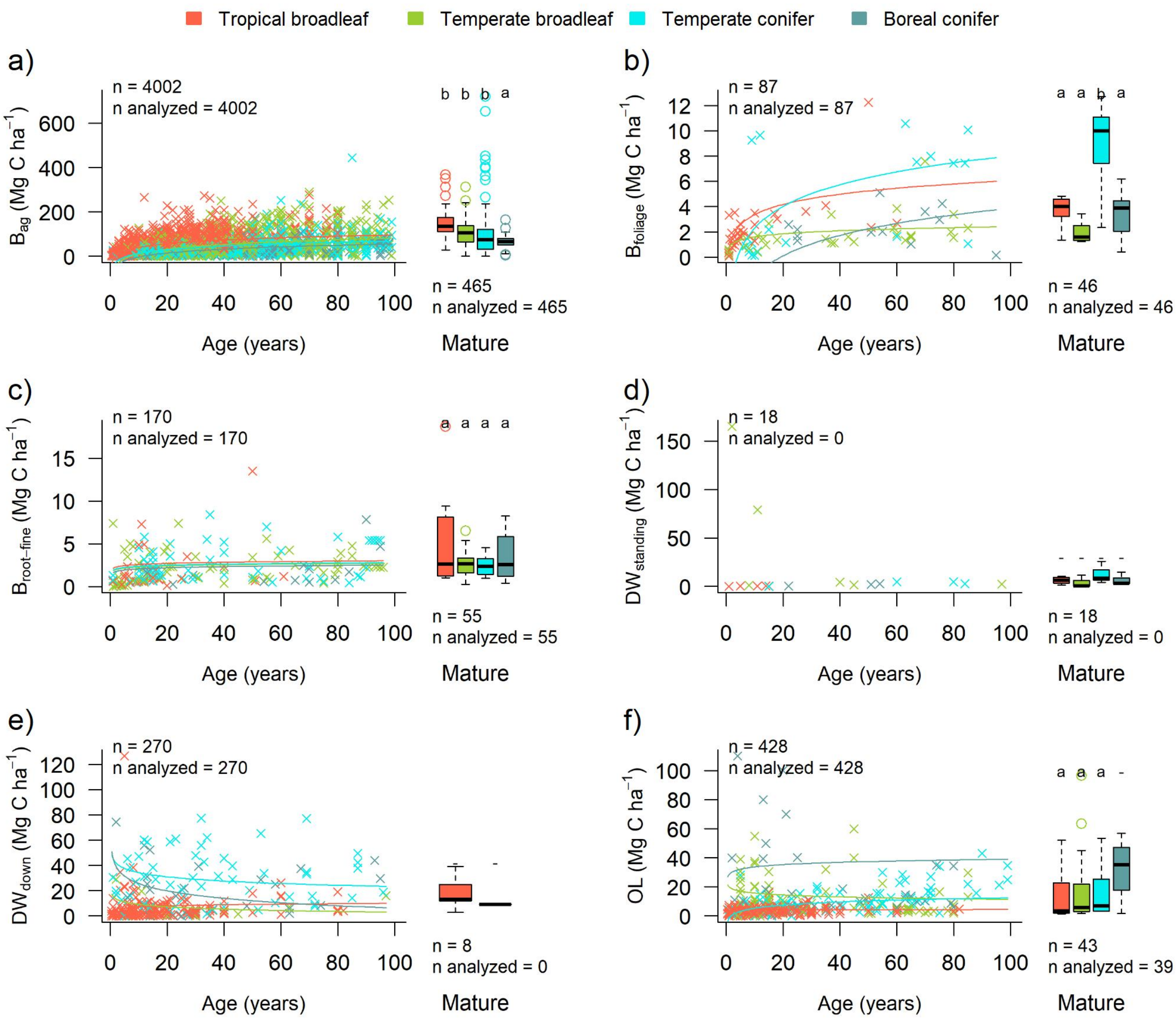

Figure 8 | Age trends and biome differences in some of the major forest C stocks: (a) B_{ag}, (b) $B_{foliage}$, (c) $B_{root-fine}$, (d) $DW_{standing}$, (e) DW_{down}, and (f) OL. The scatterplots show age trends in forests up to 100 years old, as characterized by a linear mixed effects model with fixed effects of log10(age) and biome. The fitted lines indicate the effect of age (solid lines: significant at $p<0.05$, dashed lines: non-significant), and non-parallel lines indicate a significant log10(age) x biome interaction (all variables but DW_{down}). The boxplots illustrate variation among biomes in mature forests, with different letters indicating significant differences between biomes. Data from biomes that did not meet the sample size criteria (see Methods) are plotted, but lack regression lines (young forests) or tests of differences across biomes (mature forests, indicated by a dash instead of a letter above the box plot). Individual figures for each stock with sufficient data, along with maps showing geographic distribution of the data, are given in the Supplement (Figs. S20-S30).

C cycling in young forests

C fluxes commonly increased significantly with stand age (Tables 1, S2, Figs. 7, 9, S5-S30). *ForC* contained 16 C flux variables with sufficient data to analyze age trends in young forests (see Methods). Of these, ten increased significantly with $log10[age]$: NEP, GPP, $ANPP$, $ANPP_{woody}$, $ANPP_{foliage}$, $ANPP_{litterfal}$, $BNPP$, $BNPP_{fine}$, R_{eco}, and R_{root}. The remaining six – NPP, $ANPP_{stem}$, $ANPP_{branch}$, $BNPP_{coarse}$, R_{soil}, and $R_{het-soil}$ – displayed no significant relationship to stand age.

Differences among biomes in regrowth forest C fluxes typically paralleled those observed for mature forests, with C cycling generally most rapid in the tropics and slowest in boreal forests (Table 1, Figs. 7, S5-S30). The single exception was $ANPP_{stem}$, for which temperate broadleaf and conifer forests had flux rates similar to tropical forests. Notably, and in contrast to the lack of biome differences in NEP for mature forests (Fig. 7), the tendency for temperate forests to have greater fluxes than boreal forests held for NEP in regrowth forests (tropical forests excluded because of insufficient data).

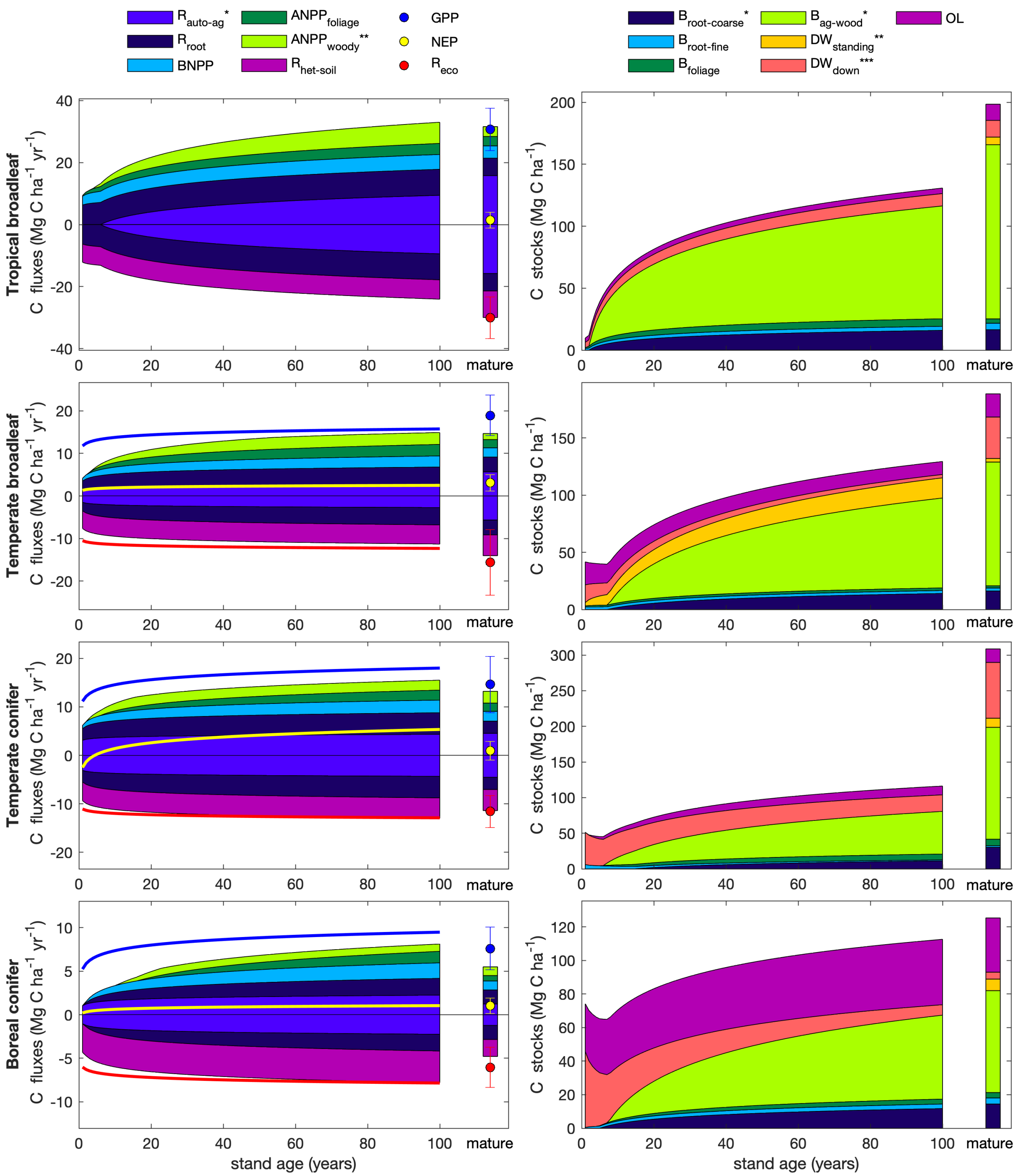

Figure 9 | Age trends in C cycling. The selection of variables for plotting seeks to maximize sample size and broad geographic representation while representing all C cycle elements. Error bars on mature forest flux estimates indicate ± 1 standard deviation. Asterisks indicate variables whose age trends were calculated based on other variables (* young and mature forests; ** young forests only; *** mature forests only), as follows. For all forests: $B_{ag-wood} = max(0, B_{ag} - B_{foliage})$, $B_{root-coarse} = max(0, B_{root} - B_{root-fine})$, $DW_{standing} = max(0, DW_{tot} - DW_{down})$. For tropical forests: $ANPP_{woody} = max(0, ANPP - ANPP_{foliage})$, $R_{auto-ag} = R_{auto} - Rroot$, where $R_{auto} = NPP(1/CUE - 1)$ and CUE=0.46 (Collati et al. 2020). For non-tropical forests: $ANPP_{woody} = min(ANPP_{stem}, ANPP_{woody})$, $R_{auto-ag} = R_{eco} - Rsoil$. Note that there remain substantial uncertainties in the functional form of age trends and discrepancies in closure among related variables.

"Closure" and internal consistency of the C flux budget were less successful for young than mature forests (Figs. 9). Summed regression equations for $R_{soil-het}$ and R_{root} were generally very close to R_{soil}. In assessing the C budget of young forests, we calculated $R_{auto-ag}$ as the difference between R_{eco} and R_{soil} (except for tropical forests, which had insufficient R_{eco} data), effectively guaranteeing near-closure of the CO_2 efflux (respiration) portion of the budget (negative values in Figs. 9). In contrast, the CO_2 influx portion of the budget generally did not "close": the sum of R_{auto} ($R_{root} + R_{auto-ag}$, as described above) and components of NPP consistently fell short of GPP, particularly in young stands (range across forest types and ages: 0.9-7.6 Mg C ha^{-1} yr^{-1}). Moreover, there was not consistent budget closure among the components of NPP, and substantially different age trends resulting from the sum of components versus total NPP (Figs. 9). Although age trends of young forests often converged towards mature forest averages, there were some discrepancies, most notably including a tendency for higher fluxes in regrowth boreal forests than in their mature counterparts (Figs. 7, 9, S5-S30).

In terms of C stocks, ten variables (all but standing deadwood, $DW_{standing}$) had sufficient data to test for age trends (Table 1, Figs. 8, S20-S30). All of these displayed a significant overall increase with the logarithm of stand age. Age × biome interactions were also significant for all ten of these C stock variables (Table S2), with living C stocks tending to accumulate more rapidly during the early stages of forest regrowth in tropical forests (Figs. 8, 9, S20-S30). In the case of two non-living C stocks (DW_{down} and OL), age × biome interactions were such that age trends were positive in some biomes and negative in others. Specifically, DW_{down} declined with age in temperate and boreal forests, compared to an increase in tropical forests (Figs. 8,9, S29). Similarly, OL declined slightly with age in temperate broadleaf forests, contrasting an increase in the other three biomes (Figs. 8, 9,S30). Again, there were some discrepancies between young forest trends and mature forests, most notably including generally higher C stocks in mature forests relative to their 100-year counterparts, particularly for temperate conifer forests (with discrepancies again driven by differences in geographic representation) and, to a lesser extent, tropical broadleaf forests (Fig. 9).

Discussion

ForC v3.0 provided unprecedented coverage of most major variables, yielding a broad picture of C cycling in the world's major forest biomes. Carbon cycling rates generally decreased from tropical to boreal climates in both mature and regrowth forests (Figs. 1, 7-9). In contrast, mature forest C stocks (biomass, dead wood, and organic layer) and NEP, which are defined by the differences between in- and out- fluxes, exhibited little systematic variation across biomes (Figs. 1, 3-6, 8). Consistent with theory and previous studies (Fig. 1b,d), the majority of autotrophic C fluxes, together with most live biomass pools, increased significantly with stand age (Table 1; Figs. 7- 9, S5-S30). Together, these results refine and expand our understanding of C cycling in mature forests, while providing the first global-scale analysis of age trends in multiple forest C stocks and fluxes (Fig. 9).

C cycling across biomes

Our analysis revealed that most C fluxes were highest in tropical forests, intermediate in temperate (broadleaf or conifer) forests, and lowest in boreal forests – a pattern that generally held for both regrowth and mature forests (Figs. 1a, 7- 9). For mature forests, this is consistent with a large body of previous work demonstrating that C fluxes generally decline with latitude and increase with temperature on a global scale (e.g., Luyssaert *et al* 2007, Gillman *et al* 2015, Li and Xiao 2019, Banbury Morgan *et al* in press). This consistency is not surprising, particularly given commonality in the data analyzed or used for calibration. The finding that these patterns hold consistently across numerous fluxes, while aligning with theoretical expectations (Fig. 1a), is novel to this analysis (but see Banbury Morgan *et al* in press for nine autotrophic fluxes).

The notable exception to the pattern of fluxes decreasing from tropical to boreal regions was NEP (the difference between GPP and R_{eco}), which showed no significant differences across biomes, albeit with the highest mean in temperate broadleaf forests (Fig. 7f). Unlike the other C flux variables, NEP does not characterize the rate at which C cycles through the ecosystem, but, as the balance between GPP and R_{eco}, represents net CO_2 sequestration (or release) by the ecosystem. NEP tends to be relatively small in mature forest stands, which accumulate carbon slowly relative to younger stands, if at all (Fig. 1a-b, Luyssaert *et al* 2008, Amiro *et al* 2010, Besnard *et al* 2018). The lack of pronounced differences across biomes is therefore consistent with both theory and previous research (e.g., Luyssaert *et al* 2007). Rather, variation in NEP of mature forests appears to be controlled less by climate and more by other factors including moderate disturbances (Curtis and Gough 2018) or disequilibrium of R_{soil} relative to C inputs (e.g., in peatlands where anoxic conditions inhibit decomposition, Wilson *et al* 2016). The fact that mature temperate broadleaf forests have a higher mean than the other biomes may reflect the fact that most of these forests are older secondary forests that, while classified here as mature, are still accumulating carbon (Curtis and Gough 2018).

In contrast to the patterns observed for NEP in mature stands, NEP of stands between 20 and 100 years of age varied across biomes, being lowest in boreal forests, intermediate in temperate broadleaf forests, and highest in temperate conifer forests (with insufficient data to assess tropical forests; Figs. 7, S5). This is consistent with findings that live biomass accumulation rates (ΔB_{ag} or ΔB_{tot}) during early secondary succession decrease with latitude (Figs. 8a, S20-S30, Anderson *et al* 2006, Cook-Patton *et al* 2020). Note, though, that NEP includes not only ΔB_{tot}, but also changes in DW_{tot}, OL, and soil carbon (not analyzed here). Biome differences in the accumulation rates of DW, OL, and soil C have not been detected, in part because these variables do not consistently increase with stand age (Figs. 1d, 8, S27-S30, and see discussion below, Cook-Patton *et al* 2020).

For regrowth forests, little was previously known about cross-biome differences in carbon fluxes, and we are not aware of any previous large-scale comparisons of C fluxes that have been limited to regrowth forests. Thus, this analysis was the first to examine flux trends in regrowth forests across biomes. The observed tendency for young forest fluxes to decrease from tropical to boreal regions paralleled patterns in mature forests (Figs. 7, 9, S5-S19), suggesting that regrowth forests follow latitudinal trends in carbon cycling similar to those of mature forests (e.g., Banbury Morgan *et al* in press).

In contrast to C fluxes and biomass accumulation rates in regrowth forests, stocks showed less systematic variation across biomes (c.f. Fig. 1c). For aboveground biomass, which is the variable in *ForC* with the broadest geographical representation, the modest trend of declining biomass from tropical to boreal regions mirrors observations from spaceborne lidar that reveal a decline in aboveground biomass (for all forests, including secondary) with latitude across the Northern hemisphere (Hu *et al* 2016). The highest-biomass forests on Earth are, however, found in coastal temperate climates of both the southern and northern hemispheres (Figs. 1c, 8a, Smithwick *et al* 2002, Keith *et al* 2009, Larjavaara and Muller-Landau 2012, Hu *et al* 2016). Disproportionate representation of forests in one such region – the US Pacific Northwest – inflated estimates of temperate conifer fluxes and stocks for some variables and was responsible for all the anomalous results described here (e.g., lack of complete C budget closure, an anomalous trend across biomes for $BNPP_{coarse}$). Thus, biome differences should always be interpreted relative to the geographic distribution of sampling, which only rarely adequately represents the majority of forested area within a biome.

Whereas aboveground biomass can be remotely sensed (albeit with significant uncertainties, Ploton *et al* 2020) and receives substantial research attention, far less is known about geographical variation in deadwood and organic layer (OL) carbon across biomes, which has proved a limitation for C accounting efforts (Pan *et al* 2011). Although these stocks can be important, exceeding 100 Mg C ha^{-1} in some stands (Figs. 8, S27-S29), this study is the first to synthesize deadwood data on a global scale (but see Cook-Patton *et al* 2020 for young forests). Unfortunately, data remain too sparse for statistical comparison across biomes (Figs. 8, S27-S29; but see below for age trends), pointing to a need for more widespread quantification of both standing and downed deadwood. *ForC* coverage of OL stocks is more comprehensive, revealing no significant differences across temperate and tropical biomes, but a tendency towards higher OL in boreal forests, consistent with the idea that proportionally slower decomposition in colder climates results in more buildup of organic matter (Fig. 1c, Allen *et al* 2002, Anderson-Teixeira *et al* 2011). Further research on non-living C stocks in the world's forests will be essential to completing the picture.

Age trends in C cycling

Our study reveals that most autotrophic C fluxes quickly increase and then decelerate as stands age (Figs. 7, 9), consistent with current understanding of age trends in forest C cycling (Fig. 1b; e.g., Magnani *et al* 2007, Amiro *et al* 2010, Anderson-Teixeira *et al* 2013). While limited records in very young (*i.e.*, <5 year old) stands resulted in poor resolution of the earliest phases of this increase for many variables (sometimes detecting no age trend; Table 1), any autotrophic C flux (e.g., GPP, NPP and its components, R_{auto}) would be minimal immediately following a stand-clearing disturbance (Fig. 1b). These would be expected to increase rapidly, along with the most metabolically active components of biomass, foliage and fine roots, which also increase rapidly with stand age (Figs. 1b,d, 7-9). In contrast, soil heterotrophic respiration

($R_{het-soil}$) and total soil respiration (R_{soil}) – and therefore R_{eco} – are expected to be non-zero following stand-clearing disturbance (Fig. 1b). These may decrease with a reduction of root respiration (R_{soil} only) and C exudates or increase in response to an influx of dead roots, DW, and OL (Bond-Lamberty *et al* 2004, Maurer *et al* 2016, Ribeiro-Kumara *et al* 2020), with the latter being strongly dependent upon the type of stand initiating disturbance (discussed below). This study detects no significant overall age trends in either $R_{het-soil}$ or R_{soil}, consistent with previous findings (Law *et al* 2003, Pregitzer and Euskirchen 2004, Goulden *et al* 2011).

Notably, net carbon sequestration (NEP) exhibits an overall increase with age across the first 100 years of stand development, with more pronounced patterns in temperate than boreal forests (Fig. 7). This finding is consistent with previous studies showing an increase in NEP across relatively young stand ages (Baldocchi *et al* 2001, Pregitzer and Euskirchen 2004, Luyssaert *et al* 2008). However, NEP is theoretically expected to peak in intermediate-aged stands and thereafter decline, consistent with decelerating C accumulation as stands age (Fig. 9, Odum 1969), and such declines have been documented (Law *et al* 2003, Luyssaert *et al* 2008). The fact that NEP values estimated by our models for 100-year-old stands were not systematically different from those of mature stands (lower for temperate broadleaf, higher for temperate conifer, and equal for boreal; Fig. 9) may be driven by differences in geographical representation across age classes or by the fitting of an inappropriate functional form. Moreover, both biomass and non-living C stocks often continue to increase well beyond the 100-yr threshold used here to delimit young and mature stands (Luyssaert *et al* 2008, Lichstein *et al* 2009, McGarvey *et al* 2014). Additional data, including on age trends of deadwood, the organic layer, and soil C will be important to parsing the timing and extend of an age-related NEP decrease across forest biomes.

In terms of stocks, our study reveals consistent increases in live biomass stocks with stand age, a pattern that is well-known and expected (e.g., Lichstein *et al* 2009, Yang *et al* 2011). This contrasts with more variable age trends in deadwood and the organic layer (Fig. 9), which depend strongly on the type of disturbance. Disturbances that remove most woody material (e.g., clearcut logging, agriculture) result in negligible deadwood in young stands, followed by a buildup over time (e.g., tropical stands in Figs. 8, 9, Vargas *et al* 2008). In contrast, natural disturbances (e.g., fire, drought, typhoons/hurricanes) can produce large amounts of deadwood (mostly $DW_{standing}$) that slowly decomposes as the stand recovers, resulting in declines across young stand ages (e.g., temperate and boreal stands in Figs. 8, 9, Carmona *et al* 2002). Further study and synthesis of non-living C stocks across biomes, stand ages, and disturbance types will be valuable in giving a more comprehensive picture.

C variable coverage and budget closure

The large number of C cycle variables covered by ForC, and the relatively high consistency among them (Figs. 3-6, 9), provide confidence that our reported mature forest means provide useful baselines for analysis. However, there is wide variation around these means, implying that any given stand could deviate substantially, and the sample means presented here probably do not represent true biome means (particularly for temperate conifer forests where high-biomass stands are over-represented in *ForC*).

In this analysis, the C cycle budgets for mature forests usually come close to closure—that is, the sums of component variables do not differ from the larger fluxes by more than one standard deviation (Figs. 3-6, 9). On the one hand, this reflects the general fact that ecosystem-scale measurements tend to close the C budget more easily and consistently than, for example, for energy balance (Stoy *et al* 2013). On the other, however, *ForC* derives data from multiple heterogeneous sources, and standard deviations within each biome are high; as a result, the standard for C closure is relatively loose (*c.f.* Houghton 2020). The one instance where the C budgets do not close according to our criteria is likely due to differences in the representation of forest types (*i.e.*, disproportionate representation of US Pacific NW for $B_{root-coarse}$ relative to B_{root}; Fig. 5) rather than issues of methodological accuracy. The overall high degree of closure implies that *ForC* gives a roughly consistent picture of C cycling within biomes for mature forests. This is an important and useful test because it allows for consistency checks within the C cycle, for example leveraging separate and independently measured fluxes to constrain errors in another (Williams *et al* 2014, Harmon *et al* 2011, Phillips *et al* 2017), or producing internally consistent global data products (Wang *et al* 2018).

In contrast, age trends for young forests generally remain less clearly defined. In large part, this is because their data records remain relatively sparse (*i.e.*, have low representation of different geographical regions for any given age) for most variables, particularly in the tropics (Anderson-Teixeira *et al* 2016). In addition, variation in the type and severity of stand-initiating disturbances introduces significant heterogeneity in both initial values and age trends of C cycle variables (e.g., Cook-Patton *et al* 2020). While this review provides the first analysis of age trends in forest C cycling for multiple variables at a global scale, improved resolution of these trends will require additional data.

There are, of course, notable holes in the ForC variable coverage that limit the scope of our inferences here. *ForC* currently has sparse–if any–coverage of fluxes to herbivores and higher consumers, along with woody mortality (M_{woody}) and DW (Table 1, Figs. S27-S29). We note that there are considerable opportunities to expand data on M_{woody} and $DW_{standing}$ through calculations from existing forest census data. *ForC* does not include soil carbon, which is covered by other efforts (e.g., Köchy *et al* 2015). *ForC* is not intended to replace databases that are specialized for particular parts of the C cycle analyses, e.g., aboveground biomass (Spawn *et al* 2020), land-atmosphere fluxes (Baldocchi *et al* 2001), soil respiration (Jian *et al* 2020), or the human footprint in global forests (Magnani *et al* 2007).

Importantly, *ForC* and the analyses presented here cover the forests that have received research attention, which are not a representative sample of the world's existing forests, either geographically or in terms of human impacts (Martin *et al* 2012). Geographically, all variables are poorly covered in Africa and Siberia (Fig. 2), a common problem in the carbon-cycle community (Schimel *et al* 2015, Xu and Shang 2016). In terms of human impacts, research efforts tend to focus on interior forest ecosystems (Martin *et al* 2012), often in permanently protected areas (e.g., Davies *et al* 2021). Studies of regrowth forests tend to focus on sites where recurring anthropogenic disturbance is not a confounding factor. Yet, fragmentation and degradation impact a large and growing proportion of Earth's forests (FAO and UNEP 2020). Fragmentation and the creation of edges strongly impact forest C cycling (e.g., Chaplin-Kramer *et al* 2015, Remy *et al* 2016, Reinmann and Hutyra 2017, Smith *et al* 2019, Ordway and Asner 2020, Reinmann *et al* 2020). Partial logging and other forms of non- stand clearing anthropogenic disturbance also alter forest C cycling (e.g., Huang and Asner 2010, Piponiot *et al* 2016), but are under-studied (Sist *et al* 2015) and excluded from this analysis. Fragmented and degraded forests do not fit the idealized conceptual framework around which this review is structured (Fig. 1), yet their representation in models, sustainability assessments, and C accounting systems is critical to accurate accounting of C cycling in Earth's forests (e.g., Huang and Asner 2010, Reinmann and Hutyra 2017, Piponiot *et al* 2019, Smith *et al* 2019). Finally, plantation forests account for approximately 3% of Earth's forests (FAO and UNEP 2020) but are not included in this analysis. While it is known that these tend to accumulate biomass faster than naturally regenerating forests (Anderson *et al* 2006, Bonner *et al* 2013), their global scale C cycling patterns remain less clearly understood (c.f. Cook-Patton *et al* 2020). Additional research and synthesis are needed to fill these critical gaps in our understanding of forest C cycling.

Relevance for climate change prediction and mitigation

The future of forest C cycling (Song *et al* 2019) will shape trends in atmospheric CO_2 and the course of climate change (Schimel *et al* 2015). Our findings, and more generally the data contained in *ForC* and summarized here, can help meet two significant challenges.

First, improved representation of forest C cycling in models is essential to improving predictions of the future course of climate change. By definition, future projections extend our existing observations and understanding to conditions that do not currently exist on Earth (Bonan and Doney 2018, Gustafson *et al* 2018, McDowell *et al* 2018). To ensure that models are giving the right answers for the right reasons (Sulman *et al* 2018), it is important to benchmark against multiple components of the C cycle that are internally consistent with each other (Collier *et al* 2018, Wang *et al* 2018). *ForC*'s tens of thousands of records are readily available in a standardized format, along with all code used in the analyses presented here. We recommend that researchers use these resources to identify and summarize data specific to the analysis at hand. Integration of *ForC* with predictive models will be valuable to improving model accuracy and reliability (Fer *et al* 2021).

Second, *ForC* can serve as a pipeline through which information can flow efficiently from forest researchers to decision-makers and practitioners working to implement forest conservation strategies at global, national, or landscape scales. This is already happening: *ForC* has contributed to updating the IPCC guidelines for carbon accounting in forests (IPCC 2019, Requena Suarez *et al* 2019), mapping C accumulation potential from natural forest regrowth globally (Cook-Patton *et al* 2020), and informing ecosystem conservation priorities (Goldstein *et al* 2020).

It is also interesting to consider the complementary utility of global-scale but spatially discontinuous databases such as ForC and wall-to-wall remote sensing products. The latter provide insight, with substantial uncertainty, into aboveground carbon stocks and GPP, but are less useful for constraining belowground stocks or carbon fluxes in general (Anav *et al* 2015, Bond-Lamberty *et al* 2016). Combining observational data and remote observations may provide a much more comprehensive and accurate picture of global forest C cycling, particularly when used in formal data assimilation systems (Liu *et al* 2018, Konings *et al* 2019). Biomass is the largest C stock in most forests, and most of the emphasis has traditionally been on this variable. Remote-sensing driven aboveground biomass estimates (e.g., Saatchi *et al* 2011), calibrated based on high-quality ground-based data (Chave *et al* 2019, Schepaschenko *et al* 2019), provide the most promising approach, but significant uncertainties remain (Ploton *et al* 2020). Note, however, that factors such as stand age and disturbance history are difficult, if not impossible, to detect remotely, and can only be characterized for recent decades (Hansen *et al* 2013, Curtis *et al* 2018, Song *et al* 2018). Ground-based data such as those in *ForC* are therefore valuable in defining age-based trajectories in biomass, as in Cook-Patton *et al* (2020), and thus constraining variables such as carbon sink potential (Luyssaert *et al* 2008).

In contrast, carbon allocation within forest ecosystems and respiration fluxes cannot be remotely sensed. Efforts such as the Global Carbon Project (Friedlingstein *et al* 2019) and NASA's Carbon Monitoring System (Liu *et al* 2018) typically compute respiration as residuals of all other terms (Harmon *et al* 2011, Bond-Lamberty *et al* 2016). This means that the errors on respiration outputs are likely to be large and certainly poorly constrained, offering a unique opportunity for databases such as ForC and SRDB (Jian *et al* 2020) to provide observational benchmarks. For example, Konings *et al* (2019) produced a top-down estimate of global heterotrophic respiration that can both be compared with extant bottom-up estimates (Bond-Lamberty 2018) and used as an internal consistency check on other parts of the carbon cycle (Phillips *et al* 2017).

Conclusions

As climate change accelerates, understanding and managing the carbon dynamics of forests– including stocks and fluxes that satellites cannot observe–is critical to forecasting, mitigation, and adaptation. The C data in *ForC*, as summarized here, are valuable to these efforts. Notably, the fact that tropical forests tend to have both the highest rates of C sequestration in young stands (Fig. 8, Cook-Patton *et al* 2020), fueled by their generally high C flux rates (Table 1; Fig. 7), and the highest mean biomass (Fig. 8, Table 1, Hu *et al* 2016, Jian *et al* 2020) reinforces the idea that conservation and restoration of these forests is a priority for climate change mitigation, along with high-biomass old-growth temperate stands (Grassi *et al* 2017, Goldstein *et al* 2020). It is also important to note the trade-off in climate mitigation potential of restoration of young forests, with high rates of CO_2 sequestration (NEP, Cook-Patton *et al* 2020), versus conservation and management of mature forests, with low NEP but high C stocks that, if lost through disturbance, could not be recovered on time scales most relevant to avoiding dangerous climate change (i.e., Goldstein *et al* 2020). Generally speaking, the conservation of mature forests will yield greater climate benefits (Anderson-Teixeira and DeLucia 2011), but both approaches are critical to avoiding catastrophic climate change (IPCC 2018).

Acknowledgements

Data availability statement

The data that support the findings of this study are openly available. Materials required to fully reproduce these analyses, including data, R scripts, and image files, are archived in Zenodo (DOI: TBD]. Data, scripts, and results presented here are also available through the open-access *ForC* GitHub repository (https://github.com/forc-db/ForC), where many will be updated as the database develops.

References

Allen A, Brown J and Gillooly J 2002 Global biodiversity, biochemical kinetics, and the energetic-equivalence rule *SCIENCE* **297** 1545–8

Amiro B D, Barr A G, Barr J G, Black T A, Bracho R, Brown M, Chen J, Clark K L, Davis K J, Desai A R, Dore S, Engel V, Fuentes J D, Goldstein A H, Goulden M L, Kolb T E, Lavigne M B, Law B E, Margolis H A, Martin T, McCaughey J H, Misson L, Montes-Helu M, Noormets A, Randerson J T, Starr G and Xiao J 2010 Ecosystem carbon dioxide fluxes after disturbance in forests of North America *J. Geophys. Res.* **115** G00K02

Anav A, Friedlingstein P, Beer C, Ciais P, Harper A, Jones C, Murray-Tortarolo G, Papale D, Parazoo N C, Peylin P, Piao S, Sitch S, Viovy N, Wiltshire A and Zhao M 2015 Spatiotemporal patterns of terrestrial gross primary production: A review *Reviews of Geophysics* **53** 785–818

Andela N, Morton D C, Giglio L, Chen Y, van der Werf G R, Kasibhatla P S, DeFries R S, Collatz G J, Hantson S, Kloster S, Bachelet D, Forrest M, Lasslop G, Li F, Mangeon S, Melton J R, Yue C and Randerson J T 2017 A human-driven decline in global burned area *Science* **356** 1356–62

Anderson K J, Allen A P, Gillooly J F and Brown J H 2006 Temperature-dependence of biomass accumulation rates during secondary succession *Ecology Letters* **9** 673–82

Anderson-Teixeira K J, Davies S J, Bennett A C, Gonzalez-Akre E B, Muller-Landau H C, Joseph Wright S, Abu Salim K, Almeyda Zambrano A M, Alonso A, Baltzer J L, Basset Y, Bourg N A, Broadbent E N, Brockelman W Y, Bunyavejchewin S, Burslem D F R P, Butt N, Cao M, Cardenas D, Chuyong G B, Clay K, Cordell S, Dattaraja H S, Deng X, Detto M, Du X, Duque A, Erikson D L, Ewango C E N, Fischer G A, Fletcher C, Foster R B, Giardina C P, Gilbert G S, Gunatilleke N, Gunatilleke S, Hao Z, Hargrove W W, Hart T B, Hau B C H, He F, Hoffman F M, Howe R W, Hubbell S P, Inman-Narahari F M, Jansen P A, Jiang M, Johnson D J, Kanzaki M, Kassim A R, Kenfack D, Kibet S, Kinnaird M F, Korte L, Kral K, Kumar J, Larson A J, Li Y, Li X, Liu S, Lum S K Y, Lutz J A, Ma K, Maddalena D M, Makana J-R, Malhi Y, Marthews T, Mat Serudin R, McMahon S M, McShea W J, Memiaghe H R, Mi X, Mizuno T, Morecroft M, Myers J A, Novotny V, de Oliveira A A, Ong P S, Orwig D A, Ostertag R, den Ouden J, Parker G G, Phillips R P, Sack L, Sainge M N, Sang W, Sri-ngernyuang K, Sukumar R, Sun I-F, Sungpalee W, Suresh H S, Tan S, Thomas S C, Thomas D W, Thompson J, Turner B L, Uriarte M, Valencia R, et al 2015 CTFS-ForestGEO : A worldwide network monitoring forests in an era of global change *Global Change Biology* **21** 528–49

Anderson-Teixeira K J, Delong J P, Fox A M, Brese D A and Litvak M E 2011 Differential responses of production and respiration to temperature and moisture drive the carbon balance across a climatic gradient in New Mexico *Global Change Biology* **17** 410–24

Anderson-Teixeira K J and DeLucia E H 2011 The greenhouse gas value of ecosystems *Global Change Biology* **17** 425–38

Anderson-Teixeira K J, Masters M D, Black C K, Zeri M, Hussain M Z, Bernacchi C J and DeLucia E H 2013 Altered Belowground Carbon Cycling Following Land-Use Change to Perennial Bioenergy Crops *Ecosystems* **16** 508–20

Anderson-Teixeira K J, Wang M M H, McGarvey J C, Herrmann V, Tepley A J, Bond-Lamberty B and LeBauer D S 2018 ForC : A global database of forest carbon stocks and fluxes *Ecology* **99** 1507–7

Anderson-Teixeira K J, Wang M M H, McGarvey J C and LeBauer D S 2016 Carbon dynamics of mature and regrowth tropical forests derived from a pantropical database (TropForC-db) *Global Change Biology* **22** 1690–709

Anderson-Teixeira K, Herrmann V, CookPatton, Ferson A and Lister K 2020 Forc-db/GROA: Release with Cook-Patton et al. 2020, Nature.

Badgley G, Anderegg L D L, Berry J A and Field C B 2019 Terrestrial gross primary production: Using NIRV to scale from site to globe *Global Change Biology* **25** 3731–40

Baldocchi D, Falge E, Gu L, Olson R, Hollinger D, Running S, Anthoni P, Bernhofer C, Davis K, Evans R, Fuentes J, Goldstein A, Katul G, Law B, Lee X, Malhi Y, Meyers T, Munger W, Oechel W, Paw K T, Pilegaard K, Schmid H P, Valentini R, Verma S, Vesala T, Wilson K and Wofsy S 2001 FLUXNET : A

New Tool to Study the Temporal and Spatial Variability of EcosystemScale Carbon Dioxide, Water Vapor, and Energy Flux Densities *Bulletin of the American Meteorological Society* **82** 2415–34

Banbury Morgan B, Herrmann V, Kunert N, Bond-Lamberty B, Muller-Landau H C and Anderson-Teixeira K J in press Global patterns of forest autotrophic carbon fluxes *Global Change Biology*

Bates D, Mächler M, Bolker B and Walker S 2015 Fitting Linear Mixed-Effects Models Using **Lme4** *Journal of Statistical Software* **67**

Besnard S, Carvalhais N, Arain M A, Black A, de Bruin S, Buchmann N, Cescatti A, Chen J, Clevers J G P W, Desai A R, Gough C M, Havrankova K, Herold M, Hörtnagl L, Jung M, Knohl A, Kruijt B, Krupkova L, Law B E, Lindroth A, Noormets A, Roupsard O, Steinbrecher R, Varlagin A, Vincke C and Reichstein M 2018 Quantifying the effect of forest age in annual net forest carbon balance *Environmental Research Letters* **13** 124018

Bonan G B 2008 Forests and Climate Change: Forcings, Feedbacks, and the Climate Benefits of Forests *Science* **320** 1444–9

Bonan G B and Doney S C 2018 Climate, ecosystems, and planetary futures: The challenge to predict life in Earth system models *Science* **359**

Bonan G B, Lombardozzi D L, Wieder W R, Oleson K W, Lawrence D M, Hoffman F M and Collier N 2019 Model Structure and Climate Data Uncertainty in Historical Simulations of the Terrestrial Carbon Cycle (1850) *Global Biogeochemical Cycles* **33** 1310–26

Bond-Lamberty B 2018 New Techniques and Data for Understanding the Global Soil Respiration Flux *Earth's Future* **6** 1176–80

Bond-Lamberty B, Epron D, Harden J, Harmon M E, Hoffman F, Kumar J, David McGuire A and Vargas R 2016 Estimating heterotrophic respiration at large scales: Challenges, approaches, and next steps *Ecosphere* **7**

Bond-Lamberty B and Thomson A 2010 A global database of soil respiration data *Biogeosciences* **7** 1915–26

Bond-Lamberty B, Wang C and Gower S T 2004 Contribution of root respiration to soil surface CO2 flux in a boreal black spruce chronosequence *Tree Physiology* **24** 1387–95

Bonner M T L, Schmidt S and Shoo L P 2013 A meta-analytical global comparison of aboveground biomass accumulation between tropical secondary forests and monoculture plantations *Forest Ecology and Management* **291** 73–86

Carmona M R, Armesto J J, Aravena J C and Pérez C A 2002 Coarse woody debris biomass in successional and primary temperate forests in Chiloé Island, Chile *Forest Ecology and Management* **164** 265–75

Cavaleri M A, Reed S C, Smith W K and Wood T E 2015 Urgent need for warming experiments in tropical forests *Global Change Biology* **21** 2111–21

Chapin F, Woodwell G, Randerson J, Rastetter E, Lovett G, Baldocchi D, Clark D, Harmon M, Schimel D, Valentini R, Wirth C, Aber J, Cole J, Goulden M, Harden J, Heimann M, Howarth R, Matson P, McGuire A, Melillo J, Mooney H, Neff J, Houghton R, Pace M, Ryan M, Running S, Sala O, Schlesinger W and Schulze E D 2006 Reconciling Carbon-cycle Concepts, Terminology, and Methods *Ecosystems* **9** 1041–50

Chaplin-Kramer R, Ramler I, Sharp R, Haddad N, Gerber J, West P, Mandle L, Engstrom P, Baccini A, Sim S, Mueller C and King H 2015 Degradation in carbon stocks near tropical forest edges *Nature Communications* **6**

Chave J, Davies S J, Phillips O L, Lewis S L, Sist P, Schepaschenko D, Armston J, Baker T R, Coomes D, Disney M, Duncanson L, Hérault B, Labrière N, Meyer V, Réjou-Méchain M, Scipal K and Saatchi S 2019 Ground Data are Essential for Biomass Remote Sensing Missions *Surveys in Geophysics*

Chave J, Réjou-Méchain M, Búrquez A, Chidumayo E, Colgan M S, Delitti W B C, Duque A, Eid T, Fearnside P M, Goodman R C, Henry M, Martínez-Yrízar A, Mugasha W A, Muller-Landau H C, Mencuccini M, Nelson B W, Ngomanda A, Nogueira E M, Ortiz-Malavassi E, Pélissier R, Ploton P, Ryan C M, Saldarriaga J G and Vieilledent G 2014 Improved allometric models to estimate the aboveground biomass of tropical trees *Global Change Biology* **20** 3177–90

Clark D A, Asao S, Fisher R, Reed S, Reich P B, Ryan M G, Wood T E and Yang X 2017 Field data to benchmark the carbon-cycle models for tropical forests *Biogeosciences Discussions* 1–44

Clark D A, Brown S, Kicklighter D W, Chambers J, Thomlinson J R and Ni J 2001 Measuring net primary production in forests: Concepts and field methods *Ecological Applications* **11** 356–70

Collalti A, Ibrom A, Stockmarr A, Cescatti A, Alkama R, Fernández-Martínez M, Matteucci G, Sitch S, Friedlingstein P, Ciais P, Goll D S, Nabel J E M S, Pongratz J, Arneth A, Haverd V and Prentice I C 2020 Forest production efficiency increases with growth temperature *Nature Communications* **11** 5322

Collier N, Hoffman F M, Lawrence D M, Keppel-Aleks G, Koven C D, Riley W J, Mu M and Randerson J T 2018 The International Land Model Benchmarking (ILAMB) System: Design, Theory, and Implementation *Journal of Advances in Modeling Earth Systems* **10** 2731–54

Cook-Patton S C, Leavitt S M, Gibbs D, Harris N L, Lister K, Anderson-Teixeira K J, Briggs R D, Chazdon R L, Crowther T W, Ellis P W, Griscom H P, Herrmann V, Holl K D, Houghton R A, Larrosa C, Lomax G, Lucas R, Madsen P, Malhi Y, Paquette A, Parker J D, Paul K, Routh D, Roxburgh S, Saatchi S, van den Hoogen J, Walker W S, Wheeler C E, Wood S A, Xu L and Griscom B W 2020 Mapping carbon accumulation potential from global natural forest regrowth *Nature* **585** 545–50

Corman J R, Collins S L, Cook E M, Dong X, Gherardi L A, Grimm N B, Hale R L, Lin T, Ramos J, Reichmann L G and Sala O E 2019 Foundations and Frontiers of Ecosystem Science: Legacy of a Classic Paper (Odum 1969) *Ecosystems* **22** 1160–72

Curtis P G, Slay C M, Harris N L, Tyukavina A and Hansen M C 2018 Classifying drivers of global forest loss *Science* **361** 1108–11

Curtis P S and Gough C M 2018 Forest aging, disturbance and the carbon cycle *New Phytologist*

Davies S J, Abiem I, Abu Salim K, Aguilar S, Allen D, Alonso A, Anderson-Teixeira K, Andrade A, Arellano G, Ashton P S, Baker P J, Baker M E, Baltzer J L, Basset Y, Bissiengou P, Bohlman S, Bourg N A, Brockelman W Y, Bunyavejchewin S, Burslem D F R P, Cao M, Cárdenas D, Chang L-W, Chang-Yang C-H, Chao K-J, Chao W-C, Chapman H, Chen Y-Y, Chisholm R A, Chu C, Chuyong G, Clay K, Comita L S, Condit R, Cordell S, Dattaraja H S, de Oliveira A A, den Ouden J, Detto M, Dick C, Du X, Duque Á, Ediriweera S, Ellis E C, Obiang N L E, Esufali S, Ewango C E N, Fernando E S, Filip J, Fischer G A, Foster R, Giambelluca T, Giardina C, Gilbert G S, Gonzalez-Akre E, Gunatilleke I A U N, Gunatilleke C

V S, Hao Z, Hau B C H, He F, Ni H, Howe R W, Hubbell S P, Huth A, Inman-Narahari F, Itoh A, Janík D, Jansen P A, Jiang M, Johnson D J, Jones F A, Kanzaki M, Kenfack D, Kiratiprayoon S, Král K, Krizel L, Lao S, Larson A J, Li Y, Li X, Litton C M, Liu Y, Liu S, Lum S K Y, Luskin M S, Lutz J A, Luu H T, Ma K, Makana J-R, Malhi Y, Martin A, McCarthy C, McMahon S M, McShea W J, Memiaghe H, Mi X, Mitre D, Mohamad M, et al 2021 ForestGEO: Understanding forest diversity and dynamics through a global observatory network *Biological Conservation* **253** 108907

DeLucia E H, Drake J, Thomas R B and Gonzalez-Meler M A 2007 Forest carbon use efficiency: Is respiration a constant fraction of gross primary production? *Global Change Biology* **13** 1157–67

Di Vittorio A V, Shi X, Bond-Lamberty B, Calvin K and Jones A 2020 Initial Land Use/Cover Distribution Substantially Affects Global Carbon and Local Temperature Projections in the Integrated Earth System Model *Global Biogeochemical Cycles* **34**

FAO 2010 *Global Forest Resources Assessment 2010* (Rome, Italy: Food and Agriculture Organization of the United Nations)

FAO and UNEP 2020 *The State of the World's Forests 2020: Forests, biodiversity and people* (Rome, Italy: FAO and UNEP)

Fer I, Gardella A K, Shiklomanov A N, Campbell E E, Cowdery E M, Kauwe M G D, Desai A, Duveneck M J, Fisher J B, Haynes K D, Hoffman F M, Johnston M R, Kooper R, LeBauer D S, Mantooth J, Parton W J, Poulter B, Quaife T, Raiho A, Schaefer K, Serbin S P, Simkins J, Wilcox K R, Viskari T and Dietze M C 2021 Beyond ecosystem modeling: A roadmap to community cyberinfrastructure for ecological data-model integration *Global Change Biology* **27** 13–26

Friedlingstein P, Cox P, Betts R, Bopp L, von Bloh W, Brovkin V, Cadule P, Doney S, Eby M, Fung I, Bala G, John J, Jones C, Joos F, Kato T, Kawamiya M, Knorr W, Lindsay K, Matthews H D, Raddatz T, Rayner P, Reick C, Roeckner E, Schnitzler K-G, Schnur R, Strassmann K, Weaver A J, Yoshikawa C and Zeng N 2006 ClimateCarbon Cycle Feedback Analysis: Results from the C4MIP Model Intercomparison *Journal of Climate* **19** 3337–53

Friedlingstein P, Jones M W, O'Sullivan M, Andrew R M, Hauck J, Peters G P, Peters W, Pongratz J, Sitch S, Quéré C L, Bakker D C E, Canadell J G, Ciais P, Jackson R B, Anthoni P, Barbero L, Bastos A, Bastrikov V, Becker M, Bopp L, Buitenhuis E, Chandra N, Chevallier F, Chini L P, Currie K I, Feely R A, Gehlen M, Gilfillan D, Gkritzalis T, Goll D S, Gruber N, Gutekunst S, Harris I, Haverd V, Houghton R A, Hurtt G, Ilyina T, Jain A K, Joetzjer E, Kaplan J O, Kato E, Klein Goldewijk K, Korsbakken J I, Landschützer P, Lauvset S K, Lefèvre N, Lenton A, Lienert S, Lombardozzi D, Marland G, McGuire P C, Melton J R, Metzl N, Munro D R, Nabel J E M S, Nakaoka S-I, Neill C, Omar A M, Ono T, Peregon A, Pierrot D, Poulter B, Rehder G, Resplandy L, Robertson E, Rödenbeck C, Séférian R, Schwinger J, Smith N, Tans P P, Tian H, Tilbrook B, Tubiello F N, Werf G R van der, Wiltshire A J and Zaehle S 2019 Global Carbon Budget 2019 *Earth System Science Data* **11** 1783–838

Gillman L N, Wright S D, Cusens J, McBride P D, Malhi Y and Whittaker R J 2015 Latitude, productivity and species richness *Global Ecology and Biogeography* **24** 107–17

Goldstein A, Turner W R, Spawn S A, Anderson-Teixeira K J, Cook-Patton S, Fargione J, Gibbs H K, Griscom B, Hewson J H, Howard J F, Ledezma J C, Page S, Koh L P, Rockström J, Sanderman J and Hole D G 2020 Protecting irrecoverable carbon in Earth's ecosystems *Nature Climate Change* **10** 287–95

Goulden M L, McMillan A M S, Winston G C, Rocha A V, Manies K L, Harden J W and Bond-Lamberty B P 2011 Patterns of NPP, GPP, respiration, and NEP during boreal forest succession *Global Change Biology* **17** 855–71

Grassi G, House J, Dentener F, Federici S, den Elzen M and Penman J 2017 The key role of forests in meeting climate targets requires science for credible mitigation *Nature Climate Change* **7** 220–6

Griscom B W, Adams J, Ellis P W, Houghton R A, Lomax G, Miteva D A, Schlesinger W H, Shoch D, Siikamäki J V, Smith P, Woodbury P, Zganjar C, Blackman A, Campari J, Conant R T, Delgado C, Elias P, Gopalakrishna T, Hamsik M R, Herrero M, Kiesecker J, Landis E, Laestadius L, Leavitt S M, Minnemeyer S, Polasky S, Potapov P, Putz F E, Sanderman J, Silvius M, Wollenberg E and Fargione J 2017 Natural climate solutions *Proceedings of the National Academy of Sciences* **114** 11645–50

Gustafson E J, Kubiske M E, Miranda B R, Hoshika Y and Paoletti E 2018 Extrapolating plot-scale CO2 and ozone enrichment experimental results to novel conditions and scales using mechanistic modeling *Ecological Processes* **7** 31

Hansen M C, Potapov P V, Moore R, Hancher M, Turubanova S A, Tyukavina A, Thau D, Stehman S V, Goetz S J, Loveland T R, Kommareddy A, Egorov A, Chini L, Justice C O and Townshend J R G 2013 High-Resolution Global Maps of 21st-Century Forest Cover Change *Science* **342** 850–3

Harmon M E, Bond-Lamberty B, Tang J and Vargas R 2011 Heterotrophic respiration in disturbed forests: A review with examples from North America *Journal of Geophysical Research* **116**

Harmon M E, Franklin J F, Swanson F J, Sollins P, Gregory S V, Lattin J D, Anderson N H, Cline S P, Aumen N G, Sedell J R, Lienkaemper G W, Cromack K and Cummins K W 1986 Ecology of Coarse Woody Debris in Temperate Ecosystems *Advances in Ecological Research* vol 15, ed A MacFadyen and E D Ford (Academic Press) pp 133–302

Harris N L, Gibbs D A, Baccini A, Birdsey R A, Bruin S de, Farina M, Fatoyinbo L, Hansen M C, Herold M, Houghton R A, Potapov P V, Suarez D R, Roman-Cuesta R M, Saatchi S S, Slay C M, Turubanova S A and Tyukavina A 2021 Global maps of twenty-first century forest carbon fluxes *Nature Climate Change* 1–7

Holdridge L R 1947 Determination of World Plant Formations From Simple Climatic Data *Science* **105** 367–8

Houghton R A 2020 Terrestrial fluxes of carbon in GCP carbon budgets *Global Change Biology* **26** 3006–14

Hu T, Su Y, Xue B, Liu J, Zhao X, Fang J and Guo Q 2016 Mapping Global Forest Aboveground Biomass with Spaceborne LiDAR, Optical Imagery, and Forest Inventory Data *Remote Sensing* **8** 565

Huang M and Asner G P 2010 Long-term carbon loss and recovery following selective logging in Amazon forests *Global Biogeochemical Cycles* **24**

Humboldt A von and Bonpland A 1807 *Essay on the Geography of Plants*

Hursh A, Ballantyne A, Cooper L, Maneta M, Kimball J and Watts J 2017 The sensitivity of soil respiration to soil temperature, moisture, and carbon supply at the global scale *Global Change Biology* **23** 2090–103

IPCC 2019 *2019 Refinement to the 2006 IPCC Guidelines for National Greenhouse Gas Inventories*

IPCC 2018 *Global Warming of 1.5C. An IPCC Special Report on the impacts of global warming of 1.5C above pre-industrial levels and related global greenhouse gas emission pathways, in the context of strengthening the global response to the threat of climate change, sustainable development, and efforts to eradicate poverty [Masson-Delmotte, V., P. Zhai, H.-O. Pörtner, D. Roberts, J. Skea, P.R. Shukla, A. Pirani, W. Moufouma-Okia, C. Péan, R. Pidcock, S. Connors, J.B.R. Matthews, Y. Chen, X. Zhou, M.I. Gomis, E. Lonnoy, T. Maycock, M. Tignor, and T. Waterfield (eds.)].*

Jian J, Vargas R, Anderson-Teixeira K, Stell E, Herrmann V, Horn M, Kholod N, Manzon J, Marchesi R, Paredes D and Bond-Lamberty B 2020 *A restructured and updated global soil respiration database (SRDB-V5)* (Data, Algorithms, and Models)

Johnson C M, Zarin D J and Johnson A H 2000 Post-disturbance aboveground biomass accumulation in global secondary forests *Ecology* **81** 1395–401

Johnson D J, Needham J, Xu C, Massoud E C, Davies S J, Anderson-Teixeira K J, Bunyavejchewin S, Chambers J Q, Chang-Yang C-H, Chiang J-M, Chuyong G B, Condit R, Cordell S, Fletcher C, Giardina C P, Giambelluca T W, Gunatilleke N, Gunatilleke S, Hsieh C-F, Hubbell S, Inman-Narahari F, Kassim A R, Katabuchi M, Kenfack D, Litton C M, Lum S, Mohamad M, Nasardin M, Ong P S, Ostertag R, Sack L, Swenson N G, Sun I F, Tan S, Thomas D W, Thompson J, Umaña M N, Uriarte M, Valencia R, Yap S, Zimmerman J, McDowell N G and McMahon S M 2018 Climate sensitive size-dependent survival in tropical trees *Nature Ecology & Evolution* 1

Jung M, Henkel K, Herold M and Churkina G 2006 Exploiting synergies of global land cover products for carbon cycle modeling *Remote Sensing of Environment* **101** 534–53

Keith H, Mackey B G and Lindenmayer D B 2009 Re-evaluation of forest biomass carbon stocks and lessons from the world's most carbon-dense forests *Proceedings of the National Academy of Sciences* **106** 11635–40

Konings A G, Bloom A A, Liu J, Parazoo N C, Schimel D S and Bowman K W 2019 Global satellite-driven estimates of heterotrophic respiration *Biogeosciences* **16** 2269–84

Köchy M, Hiederer R and Freibauer A 2015 Global distribution of soil organic carbon Part 1: Masses and frequency distributions of SOC stocks for the tropics, permafrost regions, wetlands, and the world *SOIL* **1** 351–65

Krause A, Pugh T A M, Bayer A D, Li W, Leung F, Bondeau A, Doelman J C, Humpenöder F, Anthoni P, Bodirsky B L, Ciais P, Müller C, Murray-Tortarolo G, Olin S, Popp A, Sitch S, Stehfest E and Arneth A 2018 Large uncertainty in carbon uptake potential of land-based climate-change mitigation efforts *Global Change Biology* **24** 3025–38

Kuzyakov Y 2006 Sources of CO2 efflux from soil and review of partitioning methods *Soil Biology and Biochemistry* **38** 425–48

Larjavaara M and Muller-Landau H C 2012 Temperature explains global variation in biomass among humid old-growth forests *Global Ecology and Biogeography* **21** 998–1006

Law B E, Sun O J, Campbell J, Tuyl S V and Thornton P E 2003 Changes in carbon storage and fluxes in a chronosequence of ponderosa pine *Global Change Biology* **9** 510–24

Li X and Xiao J 2019 Mapping Photosynthesis Solely from Solar-Induced Chlorophyll Fluorescence: A Global, Fine-Resolution Dataset of Gross Primary Production Derived from OCO-2 *Remote Sensing* **11** 2563

Lichstein J W, Wirth C, Horn H S and Pacala S W 2009 Biomass Chronosequences of United States Forests: Implications for Carbon Storage and Forest Management *Old-Growth Forests* Ecological Studies ed C Wirth, G Gleixner and M Heimann (Springer Berlin Heidelberg) pp 301–41

Lieth H 1973 Primary production: Terrestrial ecosystems *Human Ecology* **1** 303–32

Liu J, Bowman K, Parazoo N C, Bloom A A, Wunch D, Jiang Z, Gurney K R and Schimel D 2018 Detecting drought impact on terrestrial biosphere carbon fluxes over contiguous US with satellite observations *Environmental Research Letters* **13** 095003

Luo Y Q, Randerson J T, Abramowitz G, Bacour C, Blyth E, Carvalhais N, Ciais P, Dalmonech D, Fisher J B, Fisher R, Friedlingstein P, Hibbard K, Hoffman F, Huntzinger D, Jones C D, Koven C, Lawrence D, Li D J, Mahecha M, Niu S L, Norby R, Piao S L, Qi X, Peylin P, Prentice I C, Riley W, Reichstein M, Schwalm C, Wang Y P, Xia J Y, Zaehle S and Zhou X H 2012 A framework for benchmarking land models *Biogeosciences* **9** 3857–74

Lutz J A, Furniss T J, Johnson D J, Davies S J, Allen D, Alonso A, Anderson-Teixeira K J, Andrade A, Baltzer J, Becker K M L, Blomdahl E M, Bourg N A, Bunyavejchewin S, Burslem D F R P, Cansler C A, Cao K, Cao M, Cárdenas D, Chang L-W, Chao K-J, Chao W-C, Chiang J-M, Chu C, Chuyong G B, Clay K, Condit R, Cordell S, Dattaraja H S, Duque A, Ewango C E N, Fischer G A, Fletcher C, Freund J A, Giardina C, Germain S J, Gilbert G S, Hao Z, Hart T, Hau B C H, He F, Hector A, Howe R W, Hsieh C-F, Hu Y-H, Hubbell S P, Inman-Narahari F M, Itoh A, Janík D, Kassim A R, Kenfack D, Korte L, Král K, Larson A J, Li Y, Lin Y, Liu S, Lum S, Ma K, Makana J-R, Malhi Y, McMahon S M, McShea W J, Memiaghe H R, Mi X, Morecroft M, Musili P M, Myers J A, Novotny V, Oliveira A de, Ong P, Orwig D A, Ostertag R, Parker G G, Patankar R, Phillips R P, Reynolds G, Sack L, Song G-Z M, Su S-H, Sukumar R, Sun I-F, Suresh H S, Swanson M E, Tan S, Thomas D W, Thompson J, Uriarte M, Valencia R, Vicentini A, Vrška T, Wang X, Weiblen G D, Wolf A, Wu S-H, Xu H, Yamakura T, Yap S and Zimmerman J K 2018 Global importance of large-diameter trees *Global Ecology and Biogeography* **27** 849–64

Luyssaert S, Inglima I, Jung M, Richardson A D, Reichstein M, Papale D, Piao S L, Schulze E-D, Wingate L, Matteucci G, Aragao L, Aubinet M, Beer C, Bernhofer C, Black K G, Bonal D, Bonnefond J-M, Chambers J, Ciais P, Cook B, Davis K J, Dolman A J, Gielen B, Goulden M, Grace J, Granier A, Grelle A, Griffis T, Grünwald T, Guidolotti G, Hanson P J, Harding R, Hollinger D Y, Hutyra L R, Kolari P, Kruijt B, Kutsch W, Lagergren F, Laurila T, Law B E, Maire G L, Lindroth A, Loustau D, Malhi Y, Mateus J, Migliavacca M, Misson L, Montagnani L, Moncrieff J, Moors E, Munger J W, Nikinmaa E, Ollinger S V, Pita G, Rebmann C, Roupsard O, Saigusa N, Sanz M J, Seufert G, Sierra C, Smith M-L, Tang J, Valentini R, Vesala T and Janssens I A 2007 CO2 balance of boreal, temperate, and tropical forests derived from a global database *Global Change Biology* **13** 2509–37

Luyssaert S, Schulze E D, Borner A, Knohl A, Hessenmoller D, Law B E, Ciais P and Grace J 2008 Old-growth forests as global carbon sinks *Nature* **455** 213

Magnani F, Mencuccini M, Borghetti M, Berbigier P, Berninger F, Delzon S, Grelle A, Hari P, Jarvis P G, Kolari P, Kowalski A S, Lankreijer H, Law B E, Lindroth A, Loustau D, Manca G, Moncrieff J B, Rayment M, Tedeschi V, Valentini R and Grace J 2007 The human footprint in the carbon cycle of temperate and boreal forests *Nature* **447** 849–51

Martin L J, Blossey B and Ellis E 2012 Mapping where ecologists work: Biases in the global distribution of terrestrial ecological observations *Frontiers in Ecology and the Environment* **10** 195–201

Martin P A, Newton A C and Bullock J M 2013 Carbon pools recover more quickly than plant biodiversity in tropical secondary forests *Proceedings of the Royal Society B: Biological Sciences* **280** 20132236–6

Maurer G E, Chan A M, Trahan N A, Moore D J P and Bowling D R 2016 Carbon isotopic composition of forest soil respiration in the decade following bark beetle and stem girdling disturbances in the Rocky Mountains *Plant, Cell & Environment* **39** 1513–23

McDowell N G, Allen C D, Anderson-Teixeira K, Aukema B H, Bond-Lamberty B, Chini L, Clark J S, Dietze M, Grossiord C, Hanbury-Brown A, Hurtt G C, Jackson R B, Johnson D J, Kueppers L, Lichstein J W, Ogle K, Poulter B, Pugh T A M, Seidl R, Turner M G, Uriarte M, Walker A P and Xu C 2020 Pervasive shifts in forest dynamics in a changing world *Science* **368**

McDowell N G, Michaletz S T, Bennett K E, Solander K C, Xu C, Maxwell R M and Middleton R S 2018 Predicting Chronic Climate-Driven Disturbances and Their Mitigation *Trends in Ecology & Evolution* **33** 15–27

McGarvey J C, Thompson J R, Epstein H E and Shugart H H 2014 Carbon storage in old-growth forests of the Mid-Atlantic: Toward better understanding the eastern forest carbon sink *Ecology* **96** 311–7

Novick K A, Biederman J A, Desai A R, Litvak M E, Moore D J P, Scott R L and Torn M S 2018 The AmeriFlux network: A coalition of the willing *Agricultural and Forest Meteorology* **249** 444–56

Odum E 1969 The strategy of ecosystem development *Science* **164** 262–70

Ordway E M and Asner G P 2020 Carbon declines along tropical forest edges correspond to heterogeneous effects on canopy structure and function *Proceedings of the National Academy of Sciences* **117** 7863–70

Pan Y, Birdsey R A, Fang J, Houghton R, Kauppi P E, Kurz W A, Phillips O L, Shvidenko A, Lewis S L, Canadell J G, Ciais P, Jackson R B, Pacala S, McGuire A D, Piao S, Rautiainen A, Sitch S and Hayes D 2011 A Large and Persistent Carbon Sink in the World's Forests *Science* **333** 988–93

Pastorello G, Trotta C, Canfora E, Chu H, Christianson D, Cheah Y-W, Poindexter C, Chen J, Elbashandy A, Humphrey M, Isaac P, Polidori D, Ribeca A, van Ingen C, Zhang L, Amiro B, Ammann C, Arain M A, Ardö J, Arkebauer T, Arndt S K, Arriga N, Aubinet M, Aurela M, Baldocchi D, Barr A, Beamesderfer E, Marchesini L B, Bergeron O, Beringer J, Bernhofer C, Berveiller D, Billesbach D, Black T A, Blanken P D, Bohrer G, Boike J, Bolstad P V, Bonal D, Bonnefond J-M, Bowling D R, Bracho R, Brodeur J, Brümmer C, Buchmann N, Burban B, Burns S P, Buysse P, Cale P, Cavagna M, Cellier P, Chen S, Chini I, Christensen T R, Cleverly J, Collalti A, Consalvo C, Cook B D, Cook D, Coursolle C, Cremonese E, Curtis P S, D'Andrea E, da Rocha H, Dai X, Davis K J, De Cinti B, de Grandcourt A, De Ligne A, De Oliveira R C, Delpierre N, Desai A R, Di Bella C M, di Tommasi P, Dolman H, Domingo F, Dong G, Dore S, Duce P, Dufrêne E, Dunn A, Dušek J, Eamus D, Eichelmann U, ElKhidir H A M, Eugster W, Ewenz C M, Ewers B, Famulari D, Fares S, Feigenwinter I, Feitz A, Fensholt R, Filippa G, Fischer M, Frank J, Galvagno M, Gharun M, et al 2020 The FLUXNET2015 dataset and the ONEFlux processing pipeline for eddy covariance data *Scientific Data* **7** 225

Phillips C L, Bond-Lamberty B, Desai A R, Lavoie M, Risk D, Tang J, Todd-Brown K and Vargas R 2017 The value of soil respiration measurements for interpreting and modeling terrestrial carbon cycling *Plant and Soil* **413** 1–25

Piponiot C, Rödig E, Putz F E, Rutishauser E, Sist P, Ascarrunz N, Blanc L, Derroire G, Descroix L, Guedes M C, Coronado E H, Huth A, Kanashiro M, Licona J C, Mazzei L, d'Oliveira M V N, Peña-Claros M, Rodney K, Shenkin A, Souza C R de, Vidal E, West T A P, Wortel V and Hérault B 2019 Can timber provision from Amazonian production forests be sustainable? *Environmental Research Letters* **14** 064014

Piponiot C, Sist P, Mazzei L, Peña-Claros M, Putz F E, Rutishauser E, Shenkin A, Ascarrunz N, de Azevedo C P, Baraloto C, França M, Guedes M, Honorio Coronado E N, d'Oliveira M V, Ruschel A R, da Silva K E, Doff Sotta E, de Souza C R, Vidal E, West T A and Hérault B 2016 Carbon recovery dynamics following disturbance by selective logging in Amazonian forests *eLife* **5** e21394

Ploton P, Mortier F, Réjou-Méchain M, Barbier N, Picard N, Rossi V, Dormann C, Cornu G, Viennois G, Bayol N, Lyapustin A, Gourlet-Fleury S and Pélissier R 2020 Spatial validation reveals poor predictive performance of large-scale ecological mapping models *Nature Communications* **11** 4540

Poorter L, Bongers F, Aide T M, Zambrano A M A, Balvanera P, Becknell J M, Boukili V, Brancalion P H S, Broadbent E N, Chazdon R L, Craven D, Almeida-Cortez J S de, Cabral G A L, Jong B H J de, Denslow J S, Dent D H, DeWalt S J, Dupuy J M, Durán S M, Espírito-Santo M M, Fandino M C, César R G, Hall J S, Hernandez-Stefanoni J L, Jakovac C C, Junqueira A B, Kennard D, Letcher S G, Licona J-C, Lohbeck M, Marín-Spiotta E, Martínez-Ramos M, Massoca P, Meave J A, Mesquita R, Mora F, Muñoz R, Muscarella R, Nunes Y R F, Ochoa-Gaona S, Oliveira A A de, Orihuela-Belmonte E, Peña-Claros M, Pérez-García E A, Piotto D, Powers J S, Rodríguez-Velázquez J, Romero-Pérez I E, Ruíz J, Saldarriaga J G, Sanchez-Azofeifa A, Schwartz N B, Steininger M K, Swenson N G, Toledo M, Uriarte M, Breugel M van, Wal H van der, Veloso M D M, Vester H F M, Vicentini A, Vieira I C G, Bentos T V, Williamson G B and Rozendaal D M A 2016 Biomass resilience of Neotropical secondary forests *Nature* **530** 211–4

Pregitzer K S and Euskirchen E S 2004 Carbon cycling and storage in world forests: Biome patterns related to forest age *Global Change Biology* **10** 2052–77

Pugh T A M, Lindeskog M, Smith B, Poulter B, Arneth A, Haverd V and Calle L 2019 Role of forest regrowth in global carbon sink dynamics *Proceedings of the National Academy of Sciences* **116** 4382–7

Reinmann A B and Hutyra L R 2017 Edge effects enhance carbon uptake and its vulnerability to climate change in temperate broadleaf forests *Proceedings of the National Academy of Sciences* **114** 107–12

Reinmann A B, Smith I A, Thompson J R and Hutyra L R 2020 Urbanization and fragmentation mediate temperate forest carbon cycle response to climate *Environmental Research Letters* **15** 114036

Remy E, Wuyts K, Boeckx P, Ginzburg S, Gundersen P, Demey A, Van Den Bulcke J, Van Acker J and Verheyen K 2016 Strong gradients in nitrogen and carbon stocks at temperate forest edges *Forest Ecology and Management* **376** 45–58

Requena Suarez D, Rozendaal D M A, Sy V D, Phillips O L, Alvarez-Dávila E, Anderson-Teixeira K, Araujo-Murakami A, Arroyo L, Baker T R, Bongers F, Brienen R J W, Carter S, Cook-Patton S C, Feldpausch T R, Griscom B W, Harris N, Hérault B, Coronado E N H, Leavitt S M, Lewis S L, Marimon B S, Mendoza A M, N'dja J K, N'Guessan A E, Poorter L, Qie L, Rutishauser E, Sist P, Sonké B, Sullivan M J P, Vilanova E, Wang M M H, Martius C and Herold M 2019 Estimating aboveground net biomass change for tropical and subtropical forests: Refinement of IPCC default rates using forest plot data *Global Change Biology* **25** 3609–24

Ribeiro-Kumara C, Köster E, Aaltonen H and Köster K 2020 How do forest fires affect soil greenhouse gas emissions in upland boreal forests? A review *Environmental Research* **184** 109328

Saatchi S S, Harris N L, Brown S, Lefsky M, Mitchard E T A, Salas W, Zutta B R, Buermann W, Lewis S L, Hagen S, Petrova S, White L, Silman M and Morel A 2011 Benchmark map of forest carbon stocks in tropical regions across three continents *Proceedings of the National Academy of Sciences* **108** 9899–904

Schepaschenko D, Chave J, Phillips O L, Lewis S L, Davies S J, Réjou-Méchain M, Sist P, Scipal K, Perger C, Herault B, Labrière N, Hofhansl F, Affum-Baffoe K, Aleinikov A, Alonso A, Amani C, Araujo-Murakami A, Armston J, Arroyo L, Ascarrunz N, Azevedo C, Baker T, Bałazy R, Bedeau C, Berry N, Bilous A M, Bilous S Y, Bissiengou P, Blanc L, Bobkova K S, Braslavskaya T, Brienen R, Burslem D F R P, Condit R, Cuni-Sanchez A, Danilina D, Torres D del C, Derroire G, Descroix L, Sotta E D, d'Oliveira M V N, Dresel C, Erwin T, Evdokimenko M D, Falck J, Feldpausch T R, Foli E G, Foster R, Fritz S, Garcia-Abril A D, Gornov A, Gornova M, Gothard-Bassébé E, Gourlet-Fleury S, Guedes M, Hamer K C, Susanty F H, Higuchi N, Coronado E N H, Hubau W, Hubbell S, Ilstedt U, Ivanov V V, Kanashiro M, Karlsson A, Karminov V N, Killeen T, Koffi J-C K, Konovalova M, Kraxner F, Krejza J, Krisnawati H, Krivobokov L V, Kuznetsov M A, Lakyda I, Lakyda P I, Licona J C, Lucas R M, Lukina N, Lussetti D, Malhi Y, Manzanera J A, Marimon B, Junior B H M, Martinez R V, Martynenko O V, Matsala M, Matyashuk R K, Mazzei L, Memiaghe H, Mendoza C, Mendoza A M, Moroziuk O V, Mukhortova L, Musa S, Nazimova D I, Okuda T, Oliveira L C, et al 2019 The Forest Observation System, building a global reference dataset for remote sensing of forest biomass *Scientific Data* **6** 1–1

Schimel D, Hargrove W, Hoffman F and MacMahon J 2007 NEON: A hierarchically designed national ecological network *Frontiers in Ecology and the Environment* **5** 59–9

Schimel D, Stephens B B and Fisher J B 2015 Effect of increasing CO_2 on the terrestrial carbon cycle *Proceedings of the National Academy of Sciences* **112** 436–41

Sist P, Rutishauser E, Peña-Claros M, Shenkin A, Hérault B, Blanc L, Baraloto C, Baya F, Benedet F, Silva K E da, Descroix L, Ferreira J N, Gourlet-Fleury S, Guedes M C, Harun I B, Jalonen R, Kanashiro M, Krisnawati H, Kshatriya M, Lincoln P, Mazzei L, Medjibé V, Nasi R, d'Oliveira M V N, Oliveira L C de, Picard N, Pietsch S, Pinard M, Priyadi H, Putz F E, Rodney K, Rossi V, Roopsind A, Ruschel A R, Shari N H Z, Souza C R de, Susanty F H, Sotta E D, Toledo M, Vidal E, West T A P, Wortel V and Yamada T 2015 The Tropical managed Forests Observatory: A research network addressing the future of tropical logged forests *Applied Vegetation Science* **18** 171–4

Smith I A, Hutyra L R, Reinmann A B, Thompson J R and Allen D W 2019 Evidence for Edge Enhancements of Soil Respiration in Temperate Forests *Geophysical Research Letters* **46** 4278–87

Smithwick E A H, Harmon M E, Remillard S M, Acker S A and Franklin J F 2002 Potential upper bounds of carbon stores in forests of the Pacific Northwest *Ecological Applications* **12** 1303–17

Song J, Wan S, Piao S, Knapp A K, Classen A T, Vicca S, Ciais P, Hovenden M J, Leuzinger S, Beier C, Kardol P, Xia J, Liu Q, Ru J, Zhou Z, Luo Y, Guo D, Adam Langley J, Zscheischler J, Dukes J S, Tang J, Chen J, Hofmockel K S, Kueppers L M, Rustad L, Liu L, Smith M D, Templer P H, Quinn Thomas R, Norby R J, Phillips R P, Niu S, Fatichi S, Wang Y, Shao P, Han H, Wang D, Lei L, Wang J, Li X, Zhang Q, Li X, Su F, Liu B, Yang F, Ma G, Li G, Liu Y, Liu Y, Yang Z, Zhang K, Miao Y, Hu M, Yan C, Zhang A, Zhong M, Hui Y, Li Y and Zheng M 2019 A meta-analysis of 1,119 manipulative experiments on terrestrial carbon-cycling responses to global change *Nature Ecology & Evolution* **3** 1309–20

Song X-P, Hansen M C, Stehman S V, Potapov P V, Tyukavina A, Vermote E F and Townshend J R 2018 Global land change from 1982 to 2016 *Nature* **560** 639–43

Spawn S A, Sullivan C C, Lark T J and Gibbs H K 2020 Harmonized global maps of above and belowground biomass carbon density in the year 2010 *Scientific Data* **7** 112

Stoy P C, Mauder M, Foken T, Marcolla B, Boegh E, Ibrom A, Arain M A, Arneth A, Aurela M, Bernhofer C, Cescatti A, Dellwik E, Duce P, Gianelle D, van Gorsel E, Kiely G, Knohl A, Margolis H, McCaughey H, Merbold L, Montagnani L, Papale D, Reichstein M, Saunders M, Serrano-Ortiz P, Sottocornola M, Spano D, Vaccari F and Varlagin A 2013 A data-driven analysis of energy balance closure across FLUXNET research sites: The role of landscape scale heterogeneity *Agricultural and Forest Meteorology* **171-172** 137–52

Sulman B N, Moore J A M, Abramoff R, Averill C, Kivlin S, Georgiou K, Sridhar B, Hartman M D, Wang G, Wieder W R, Bradford M A, Luo Y, Mayes M A, Morrison E, Riley W J, Salazar A, Schimel J P, Tang J and Classen A T 2018 Multiple models and experiments underscore large uncertainty in soil carbon dynamics *Biogeochemistry* **141** 109–23

Taylor P G, Cleveland C C, Wieder W R, Sullivan B W, Doughty C E, Dobrowski S Z and Townsend A R 2017 Temperature and rainfall interact to control carbon cycling in tropical forests ed L Liu *Ecology Letters* **20** 779–88

Team R C 2020 R : A language and environment for statistical computing. R Foundation for Statistical Computing, Vienna, Austria. URL http://www.R-project.org/.

Tubiello F N, Pekkarinen A, Marklund L, Wanner N, Conchedda G, Federici S, Rossi S and Grassi G 2020 Carbon Emissions and Removals by Forests: New Estimates 1990–2020 *Earth System Science Data Discussions* 1–21

Vargas R, Allen M F and Allen E B 2008 Biomass and carbon accumulation in a fire chronosequence of a seasonally dry tropical forest *Global Change Biology* **14** 109–24

Wang Y, Ciais P, Goll D, Huang Y, Luo Y, Wang Y-P, Bloom A A, Broquet G, Hartmann J, Peng S, Penuelas J, Piao S, Sardans J, Stocker B D, Wang R, Zaehle S and Zechmeister-Boltenstern S 2018 GOLUM-CNP v1.0: A data-driven modeling of carbon, nitrogen and phosphorus cycles in major terrestrial biomes *Geoscientific Model Development* **11** 3903–28

Warner D L, Bond-Lamberty B, Jian J, Stell E and Vargas R 2019 Spatial Predictions and Associated Uncertainty of Annual Soil Respiration at the Global Scale *Global Biogeochemical Cycles* **33** 1733–45

Williams C A, Collatz G J, Masek J, Huang C and Goward S N 2014 Impacts of disturbance history on forest carbon stocks and fluxes: Merging satellite disturbance mapping with forest inventory data in a carbon cycle model framework *Remote Sensing of Environment* **151** 57–71

Wilson R M, Hopple A M, Tfaily M M, Sebestyen S D, Schadt C W, Pfeifer-Meister L, Medvedeff C, McFarlane K J, Kostka J E, Kolton M, Kolka R K, Kluber L A, Keller J K, Guilderson T P, Griffiths N A, Chanton J P, Bridgham S D and Hanson P J 2016 Stability of peatland carbon to rising temperatures *Nature Communications* **7** 13723

Xu M and Shang H 2016 Contribution of soil respiration to the global carbon equation *Journal of Plant Physiology* **203** 16–28

Yang Y, Luo Y and Finzi A C 2011 Carbon and nitrogen dynamics during forest stand development: A global synthesis *New Phytologist* **190** 977